C. R. Palevol 18 (2019) 619–642

Contents lists available at ScienceDirect

Comptes Rendus Palevol

www.sciencedirect.com

General Palaeontology, Systematics, and Evolution (Vertebrate Palaeontology)

Fossil Giraffidae (Mammalia, Artiodactyla) from the early Turolian of Kavakdere (Central Anatolia, Turkey)

Giraffidae (Mammalia, Artiodactyla) fossiles du Turolien inférieur de Kavakdere (Anatolie centrale, Turquie)

Alexandros Xafis[a,*], Serdar Mayda[b], Friðgeir Grímsson[c], Doris Nagel[a], Tanju Kaya[d], Kazım Halaçlar[e]

[a] *Department of Paleontology, Faculty of Earth Sciences, University of Vienna, Austria*
[b] *Department of Biology, Faculty of Science, Ege University, Bornova, Izmir, Turkey*
[c] *Department of Botany and Biodiversity Research, University of Vienna, Austria*
[d] *Natural History Museum, Ege University, Bornova, Izmir, Turkey*
[e] *Institute of Vertebrate Paleontology and Paleoanthropology, Chinese Academy of Sciences and University of Chinese Academy of Sciences, Beijing, China*

ARTICLE INFO

Article history:
Received 7 February 2019
Accepted after revision 22 April 2019
Available online 25 September 2019

Handled by Lorenro Rook

Keywords:
Ruminantia
Helladotherium
Bramatherium
Palaeotragus
Alcicephalus
MN11

Mots clés :
Ruminants
Helladotherium
Bramatherium
Palaeotragus
Alcicephalus
MN11

ABSTRACT

The fossiliferous site at Kavakdere is one of many important late Miocene fossil mammal-bearing localities in Anatolia. Previous taxonomic studies on its fauna have revealed a plethora of taxa. However, the fossil Giraffidae from this early Turolian locality were until now poorly documented. New comprehensive descriptions, comparisons and metric analyses using all accessible Giraffidae specimens from Kavakdere suggest the co-occurrence of five different giraffid taxa. These include *Helladotherium duvernoyi, Bramatherium perimense* and *Palaeotragus rouenii*. Two different samotheriines are also identified; the smaller *Samotherium boissieri* and the larger *Alcicephalus neumayri*. The latter is only known from the Turolian of Iran and North China. The occurrence of *A. neumayri* at Kavakdere constitutes the first fossil record of this taxon from a western locality, suggesting a more dominant presence of *Alcicephalus* in the Pikermian biome.

RÉSUMÉ

Le site fossilifère de Kavakdere est l'une des nombreuses localités importantes d'Anatolie contenant des mammifères fossiles du Miocène supérieur. Les études taxonomiques antérieures ont révélé une pléthore de taxa. Cependant, les Giraffidae fossiles de cette localité du Turolien inférieur ont été jusqu'à présent peu documentés. De nouvelles données détaillées, des comparaisons et des analyses métriques utilisant tous les spécimens de Giraffidae accessibles de Kavakdere suggèrent la co-occurrence de cinq différents taxons

* Corresponding author.
E-mail address: alexandros.xafis@univie.ac.at (A. Xafis).

https://doi.org/10.1016/j.crpv.2019.04.010

de giraffidés. Ils incluent *Helladotherium duvernoyi, Bramatherium perimense* et *Palaeotragus rouenii*. Deux différents samothériinés sont aussi identifiés; le plus petit *Bramatherium boissieri* et le plus grand *Palaeotragus rouenii.* Ce dernier n'est connu que dans le Turolien d'Iran et de Chine du Nord. L'occurrence d'*A. neumayri* à Kavakdere constitue le premier enregistrement fossile de ce taxon dans une localité occidentale, suggérant une présence plus dominante d'*Alcicephalus* dans le biome pikermien.

1. Introduction

The fossiliferous site at Kavakdere constitutes one of numerous late Miocene Anatolian fossil mammal-bearing localities and is located approximately 65 km NNW of Ankara (Fig. 1). Previous palaeontological studies have been conducted by Ozansoy (1965), Becker-Platen et al. (1975), Köhler (1987), Geraads and Güleç (1999), Viranta and Werdelin (2003), Sen (2017) and Koufos et al., 2018. Ozansoy (1965) compiled the first faunal list for this site, which was later enriched by Becker-Platen et al. (1975). Later, Geraads and Güleç (1999) presented and described a large skull of *Bramatherium perimense* Falconer (1845) from the same locality. Their study was, in fact, the first comprehensive taxonomic work on the fossil mammals from Kavakdere, since previous studies listed only fossil taxa without a comprehensive framework, descriptions and/or illustrations. Furthermore, Viranta and Werdelin (2003) and Koufos et al. (2018) described fossil Carnivora from Kavakdere, adding *Hyaenictitherium wongii* Zdansky (1924), *Adcrocuta eximia* Roth and Wagner (1854), *Pseudaelurus* cf. *lorteti* Gaillard (1899), and a small Carnivora indet. to the existing faunal list. Lastly, Sen (2017) described the first record of a large hipparionine *Hippotherium brachypus* Hensel (1862), the chalicotheriid *Ancylotherium pentelici* Gaudry and Lartet (1856), as well as a possible occurrence of a new subspecies of *A. eximia*. Most of the above-mentioned studies were based on collections hosted in the Natural History Museum of Ankara (MTA). Nonetheless, a part of the assemblage which was collected by Dr. Ozansoy during the 1950s is hosted in the Natural History museum of Ege University, Izmir, Turkey (EUNHM).

The family Giraffidae constitutes a group of pecoran ruminants, which are characterized by the presence of bilobed canines, brachydont cheek teeth, as well as epiphyseal cranial appendages called ossicones (Grossman and Solounias, 2014; Harris et al., 2010; Janis, 1987; Solounias, 1988). Giraffids exhibit a wide geographic distribution throughout the Pikermian biome, from the early Miocene with the appearance of the first ancestral forms of giraffids (Arambourg, 1963; Harris et al., 2010; Solounias, 2007). The now extinct Pikermian biome used to extend from Spain to China and northern Africa (Danowitz et al., 2016 and literature cited therein). During the Miocene, giraffids were widespread across this area and, allegedly, inhabited sclerophyllous evergreen woodlands that were later replaced by dryer and more open habitats during the Pliocene (Danowitz et al., 2016; Solounias et al., 1999). Kavakdere, alongside numerous other Greek and Anatolian localities, is considered as part of the central region of the Pikermian biome. Herein we describe all dental and postcranial material of Giraffidae found at Kavakdere, from the historical fossil assemblage collected by Dr. Ozansoy. The giraffid material is compared to fossil elements of the respective taxa, found across the Greco-Iranian province, and analysed using both morphological and metrical data. These analyses segregate five different giraffid species from Kavakdere. All taxa are thoroughly described and illustrated herein. Furthermore, the giraffids from Kavakdere are discussed in a time-related biogeographic framework.

1.1. Locality and geological setting

Middle Miocene to Pleistocene fossiliferous sedimentary rocks in the Sinap Tepe–Beycedere–Kavakdere area, northwest of Ankara, central Anatolia, in the vicinity of the towns Kazan and Çubuk, are part of the Sinap Formation (summarized in Lunkka et al., 2003). The Sinap Formation comprises seven members (Yellidoruk Mb, Lower Sinap Mb, Middle Sinap Mb, Upper Sinap Mb, Beycedere Mb, Kavakdere Mb, Igbek Mb: see Fig. 1.3 in Lunkka et al., 2003). The basal and oldest member is the Beycedere Mb. It is overlain by the Lower to Upper Sinap Members and the contemporaneous Igbek Mb. The upper units of the Sinap Members and the Igbek Mb overlap the lower part of the successive Kavakdere Mb. All these members are of middle to late Miocene age. The following Çalta Mb is of late Miocene to Pliocene age (see Fig. 1.3 in Lunkka et al., 2003). Outcrops or sections in the Sinap Tepe–Beycedere–Kavakdere area are grouped according to their geographic position into three subareas: 1) Sinap Tepe (incl. the sections Yellidoruk I, Yellidoruk II, Delikayincak Tepe, and Sinap I to VI), 2) Igbek (incl. the Igbek section), and 3) Beycedere–Kavakdere (incl. the sections Beycedere, Kavakdere S, Kavakdere N). Sections in the Sinap Tepe subarea are characterized by the Yellidorik and Sinap Members, magnetostratigraphically correlated as 10.899–9.279 Ma and of early to middle Vallesian age (Kappelman et al., 2003: Koufos et al., 2018). The Igbek subarea is characterized by the Igbek Mb, with an interpolated age of 9.130 Ma and is of late Vallesian age (Kappelman et al., 2003: Koufos et al., 2018). The sections in the Beycedere–Kavakdere subarea are characterized by the Beycedere and Kavakdere Members. These are of early Turolian age, spanning a range from 8.866 to 8.121 Ma (Kappelman et al., 2003: Koufos et al., 2018). The giraffid collection described herein was collected from the upper units of the Kavakdere N section (Kavakdere Mb, see Fig. 1.7 in Lunkka et al., 2003). This horizon is equivalent to Loc. 26 of the latest Sinap Project, conducted by Prof. B. Alpagut during the years 1989–1995

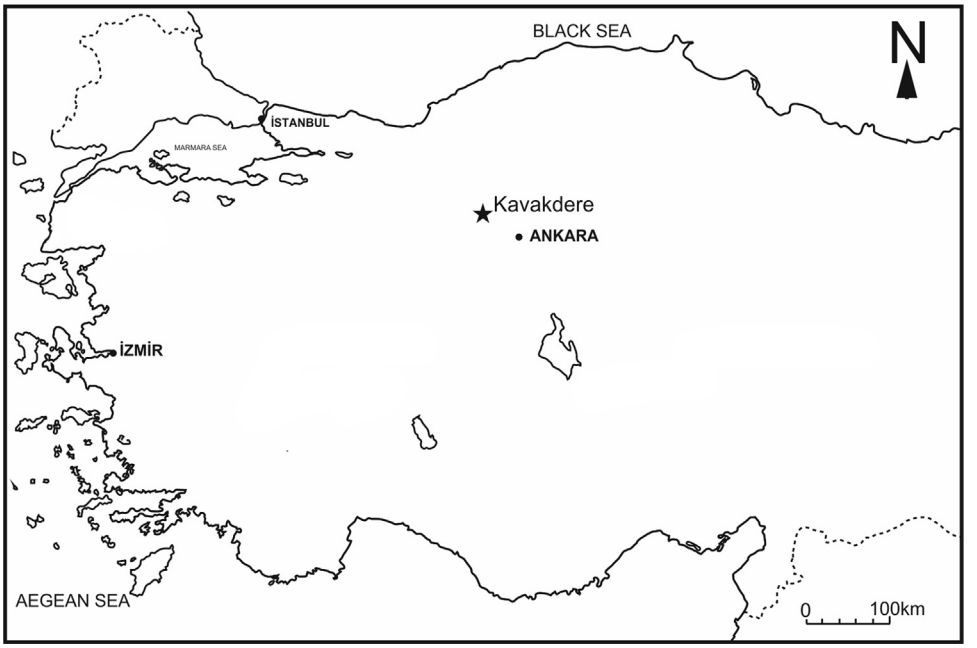

Fig. 1. Geographical map indicating the geographic position of the fossiliferous site Kavakdere (star) in relation to Ankara, Izmir, and Istanbul.
Fig. 1. Carte géographique indiquant la position géographique du site fossilifère de Kavakderen (étoile) en relation avec Ankara, Izmir et Istamboul.

(Kappelman et al., 2003; Sen, 2003). The sedimentary rock section at Kavakdere N is dominated by silicified mudstones interbedded with marly sediments in the lower part and coarser units in the upper half (Lunkka et al., 2003). The fossiliferous horizon was magnetostratigraphically dated to 8.12 Ma by Kappelman et al. (2003).

2. Materials and methods

The fossil giraffid material from AAK is stored in the Natural History Museum of Ege University, Izmir, Turkey (EUNHM). The present study focuses on fossil dental and post cranial material of Giraffidae and its main goal is to update the faunal list of AAK based on this historical collection. All material was measured using an electronic calliper, as well as a measuring tape, for the larger specimens. Measurements are given in millimetres and presented in the respective tables. Width measurements of dental elements were taken on the base of the crown. Statistical analyses were achieved using the software PAST (Hammer et al., 2001). Dental terminology follows Bärmann and Rössner (2011). Anatomical terms of postcranial elements follow Schaller (2007), Solounias and Danowitz (2016a), and Ríos et al. (2016).

2.1. Institutional and anatomical abbreviations

AAK: Ankara–Kavakdere; AMNH: American Museum of Natural History; EUNHM: Natural History Museum of Ege University, Izmir, Turkey; MTA: Natural History Museum of Ankara, Turkey; NHB: Natural History Museum of Basel; NHMW: Natural History Museum of Vienna; RIN: Rajabhat Institute Nakhon, Ratchasima; SMNS: Staatliches Museum für Naturkunde Stuttgart, Germany.

3. Systematic Palaeontology

Class Mammalia Linnaeus, 1758
Order Artiodactyla Owen, 1848
Family Giraffidae Gray, 1821
Subfamily Sivatheriinae Zittel, 1893
Genus *Helladotherium* Gaudry, 1860
Helladotherium duvernoyi (Gaudry and Lartet, 1856)

Material: PV-156, distal part of right humerus; PV-155, left radius; PV-33, distal part of left radius; PV-154, right metacarpal; PV-151, left tibia; PV-157, left astragalus; PV-158, right astragalus; PV-237, right naviculocuboideum; PV-152, right metatarsal; PV-159, proximal phalanx; PV-160, proximal phalanx; PV-161, proximal phalanx; PV-162, middle phalanx; PV-163, middle phalanx (Fig. 2; Table 1).

Descriptions: *H. duvernoyi* is represented only by postcranial elements of the front and hind limbs. The humerus (PV-156; Fig. 2A) maintains the distal condyle and most of the diaphysis, while the proximal epiphysis is absent. Medially, the teres tuberosity, for the termination of M. teres major and M. latissimus is well pronounced, narrow and long. The crista humeri is blunt and almost not visible. The radial fossa is shallow but well-defined. The fossa olecrani is open and sub-rounded. The lateral epicondyle is strong giving the lateral trochlea a quadrate shape, while the medial epicondyle is weak and blunt. The distal trochlea is asymmetrical with the medial condyle being notably smaller. In cranial aspect, the medial condyle is interrupted by a grove, which is positioned medio-caudally to the keel of the trochlea.

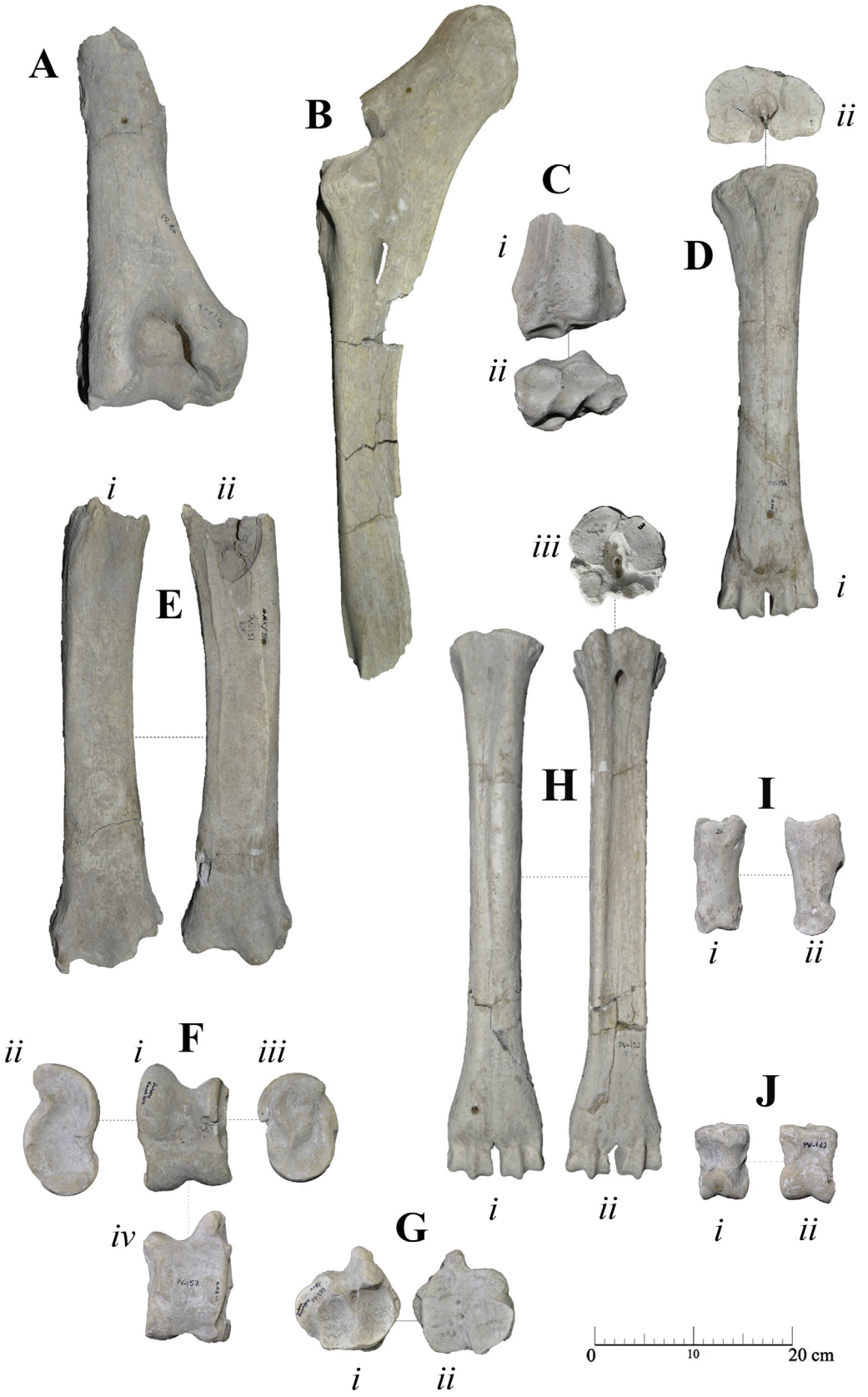
A
B
C
i
ii
D
ii
i
E
i
ii
iii
H
i
ii
I
i
ii
F
ii
i
iii
iv
J
i
ii
G
i
ii
0
10
20 cm

Two incomplete specimens of radii were recovered. PV-155 (Fig. 2B) represents a radius-ulna with the proximal part, as well as a large part of the diaphysis recovered, while PV-33 (Fig. 2C) represents only the distal part of a left radius. In proximal aspect, the medial articular surface is rounded and notably smaller than the lateral one, which shows a sub-quadrate outline. Both surfaces are wide, slightly concave and well limited by an evident and sharp rim. The lateral protuberance is well developed, but not as strong as the radial tuberosity. The diaphysis is simple, with the medial and lateral surfaces running almost parallel to each other. On the distal trochlea and in cranial aspect, the groove for the extensor carpi radialis and the common extensor tendon is wide and shallow. This area is well defined by two strong crests, which run parallel to each other from the medial plane of the scaphoid facet and the medial plane of the lunatum facet until almost the lower 25% of the length of the radius. The lateral styloid process is strong and more developed than the medial one. In distal aspect, the facet for the scaphoid is deep and rounded. The facet for the lunatum is also deep, with crests of the facet being parallel only caudally. The surface for the pyramidal is shallow and semi-circular. On PV-155, a large part of the ulna is also present. The tuber olecrani is strong, extending caudally. The processus anconeus is absent and the processus coronoideus is completely fused with the caudal plane of the head of the radius. The incisura trochlearis is long and wide. The proximal interosseous space between radius and ulna is long. The lateral and medial borders of the corpus ulnae are not visible, due to the strong fusion with the radius.

The metacarpal (PV-154; Fig. 2D) is long and robust. In palmar aspect, the medial and lateral epicondyles seem equally developed. In dorsal and proximal aspects, however, the medial epicondyle is more developed, due to the positioning of the facet for the trapezoideo-capitatum. This facet is almost rectangular, while the facet for the hamatum is sub-triangular. The epicondyles are well separated by the open synovial fossa, which is deep and extends towards the central trough, a common feature in members of the Sivatheriinae. The latter is deep and concave on the upper part of the shaft and flattens gradually towards the head of the metacarpal. The trough is limited by two strong ridges, with the medial ridge being notably sharper than the lateral ridge. The head is flat, and the keels of the distal condyles are strong and sharp in palmar aspect, getting progressively blunter towards the dorsal side.

The tibia is represented by an almost complete specimen (PV-151; Fig. 2E) with the proximal extremity being absent. The diaphysis is simple and slightly bent. In cranial aspect, the shaft is smooth and there is only a small groove noted towards the proximal end of the tibia, which would lead to the extensor groove. Caudally, the shaft is more ornamented, with a very long popliteal line originating from the distal epiphysis and running through the whole shaft, parallel to the weak curve of the tibia. Additional long muscular lines can be seen towards the lateral margin of the shaft. The medial malleolus is strongly developed. In distal aspect, the facets for the astragalus are parallel, with the lateral one being slightly larger.

Two astragali of *Helladotherium* have been recovered (PV-157, PV- 158; Fig. 2F). In dorsal aspect, the lateral ridge of the trochlea is very strong. The medial ridge is notably thinner, leading to a blunt lip on the medial margin. The medial bulge at the collum tali is fairly developed and rounded. The head is slightly asymmetrical, with the lateral trochlea being somewhat bigger than the medial trochlea. The groove of the trochlea is open, following the slight curve of the lateral ridge. The ventral articular surface is almost square in shape, with the medial margin interrupted by a distinct medial scala. The proximal triangular fossa is deep and well defined. The distal intracephalic fossa is very weak and the medial scala very prominent, a common feature observed in *Helladotherium*.

The naviculocuboideum (PV-237; Fig. 2G) is large and oval shaped in proximal view. The astragalar facets are parallel, with the lateral one being notably longer. The lateral peak is short and blunt. The calcaneal facet is long and extends almost behind the lateral peak, as in all Sivatheriinae. In distal aspect, the facet for the metatarsal is sub-triangular. The facet for the external cuneiform is almost as big as the metatarsal facet and it is sub-rectangular in shape. The facet for the medial cuneiform is much smaller, oval shaped and well separated from the medial cuneiform facet by a sharp crest.

The metatarsal (PV-152; Fig. 2H) is long and complete, revealing all distinctive features. In proximal view, the facet for the naviculocuboideum is long and is sub-rectangularly shaped. The facet for the external cuneiform is slightly larger and the facet for the medial cuneiform is small and rounded. In plantar view, the epicondyles are all strong and well separated. The dorsal head of the lateral epicondyle is rounded and robust. The ventral head of the lateral epicondyle is broken, and it seems to be as developed as the dorsal head, but less extended laterally. The medial epicondyle is generally stronger and more robust. The ventral head is very strong, leading to the blunt medial ridge of the central trough. The pygmaios is absent. On the distal epiphysis, the keels of the medial and the lateral condyles are strong and equally developed in plantar and dorsal aspect.

Fig. 2. Fossil post-cranial material of *Helladotherium duvernoyi* from Kavakdere. A: PV-156, distal part of right humerus; B: PV-155, left radius; C: PV-33, distal part of left radius, (i) cranial view and (ii) distal view; D: PV-154, right metacarpal, (i) dorsal view and (ii) proximal view; E: PV-151, left tibia, (i) cranial view and (ii) caudal view; F: PV-157, left astragalus, (i) dorsal view, (ii) lateral view, (iii) medial view and (iv) plantar view; G: PV-237, right naviculocuboideum, (i) proximal view and (ii) distal view; H: PV-152, right metatarsal, (i) dorsal view, (ii) plantar view and (iii) proximal view; I: PV-159, first phalanx, (i) dorsal view and (ii) lateral view; J: PV-162, second phalanx, (i) dorsal view and (ii) plantar view. The scale equals 20 centimetres.
Fig. 2. Matériel post-crânien fossile d'*Helladotherium duvernoyi* de Kavakdere. A : PV-156, partie distal d'humérus droit ; B : PV-155, radius gauche ; C : PV-33, partie distale de radius gauche, vues crânienne (i) et distale (ii) ; D : PV-154, métacarpien droit, vues dorsale (i) et proximale (ii) ; E : PV-151, tibia gauche, vues crânienne (i) et caudale (ii) ; F : PV-157, astragale gauche, vues dorsale (i), latérale (ii), médiale (iii) et plantaire (iv) ; G : PV-237, naviculocuboideum, vues proximale (i) et distale (ii) ; H : PV-152, métatarse droit ; vues dorsale (i), plantaire (ii) et proximale (iii) ; I : PV-159, première phalange, vue dorsale (i) et latérale (ii) ; J : PV-162, seconde phalange, vues dorsale (i) et plantaire (ii). Échelle = 20 cm.

Table 1
Measurements of post-cranial elements of *Helladotherium duvernoyi* from Kavakdere. Sin: left; Dex: right; TD: transverse diameter; APD: antero-posterior diameter; L: length; prox: proximal; dia: diaphysis; dis: distal; d: width of the ulnar articulation surface; lat: lateral; med: medial; Hmax: maximum height; H1: Height of the cubonavicular on the level of the medial astragalar surface; H2: Height of the cubonavicular on the level of the lateral astragalar surface. All measurements given in millimetres.

Tableau 1
Mesures des éléments post-crâniens d'*Helladotherium duvernoyi* de Kavakdere. Sin : gauche ; Dex : droite ; TD : diamètre transversal ; APD : diamètre antéro-postérieur ; L : longueur ; prox : proximal ; dia : diaphyse ; dis : distal ; d : largeur de la surface articulaire de l'ulna ; lat : latéral ; med : médial ; Hmax : hauteur maximum ; H1 : hauteur du cubonaviculaire au niveau de la surface médiale de l'astragale ; H2 : hauteur du cubonaviculaiure au niveau de la surface latérale de l'astragale. Toutes les mesures sont en millimètres.

Humerus

Inv. Number	Taxon	Sin/Dex	TDdia	APDdia	Tddis	APDdis
PV-156	*Helladotherium duvernoyi*	dex	75.16	76.6	141.71	135.86

Radius-Ulna

Inv. Number	Taxon	Sin/Dex	d	TDprox	APDprox	TDdia	APDdia	TDdis	APDdis
PV-155	*Helladotherium duvernoyi*	sin	76.86	153.25	80.18	81.36	80.93		
PV-33	*Helladotherium duvernoyi*	sin						102.42	73.02

Metacarpus

Inv. Number	Taxon	Sin/Dex	L	TDprox	APDprox	TDdia	APDdia	Tddis	APDdis
PV-154	*Helladotherium duvernoyi*	dex	415.2	101.73	67.33	57.82	50.56	98.77	62.78

Tibia

Inv. Number	Taxon	Sin/Dex	TDdia	APDdia	TDdis	APDdis
PV-151	*Helladotherium duvernoyi*	sin	70.52	53.78	110.08	80.03

Astragalus

Inv. Number	Taxon	Sin/Dex	Llat	Lmed	TDprox	TDdis
PV-157	*Helladotherium duvernoyi*	sin	110.26	90.89	69.77	69.7
PV-158	*Helladotherium duvernoyi*	dex	114.51	99.48	80.95	76.58

Naviculocuboideum

Inv. Number	Taxon	Sin/Dex	TD	APDmed	APDmax	Hmax	H1	H2
PV-237	*Helladotherium duvernoyi*	dex	88.66	71.62	92.3	64.07	25.18	33.26

Metatarsus

Inv. Number	Taxon	Sin/Dex	L	TDprox	APDprox	TDdia	APDdia	TDdis	APDdis
PV-152	*Helladotherium duvernoyi*	dex	432.44	78.02	76.54	42.52	48.08	79.34	48.72

Phalanx 1

Inv. Number	Taxon	L	TDprox	APDprox	TDdis	APDdis
PV-159	*Helladotherium duvernoyi*	108.32	47	50.82	45.46	36.2
PV-160	*Helladotherium duvernoyi*	108.54	45.36	47.36	40.11	32.34
PV-161	*Helladotherium duvernoyi*	107.56	48.47	52.83	42.77	33.2

Phalanx 2

Inv. Number	Taxon	L	TDprox	APDprox	TDdis	APDdis
PV-162	*Helladotherium duvernoyi*	62.23	42.73	45.82	39.44	46.82
PV-163	*Helladotherium duvernoyi*	58.82	42.6	45.41	39.61	46.49

The proximal phalanx (PV-159, PV-160, PV-161; Fig. 2I) is robust. The medial and lateral margins of the body are almost parallel to each other, since the base and the head of the phalanx are only slightly extended mediolaterally. On the articular fovea, the medial articular facet is well separated by the larger lateral articular facet by a distinct trough. In lateral and medial view, the palmar tubercles are strong and long, typical for the taxon. The head of the phalanx is asymmetrical, with the medial trochlea being slightly bigger than the lateral trochlea.

The middle phalanx (PV-162, PV-163; Fig. 2J) is short, with an almost flat palmar surface and a strongly convex plantar margin. The palmar tubercles are robust and postero-dorsally extended. The medial and lateral keels of the distal epiphysis are sharp and well-defined.

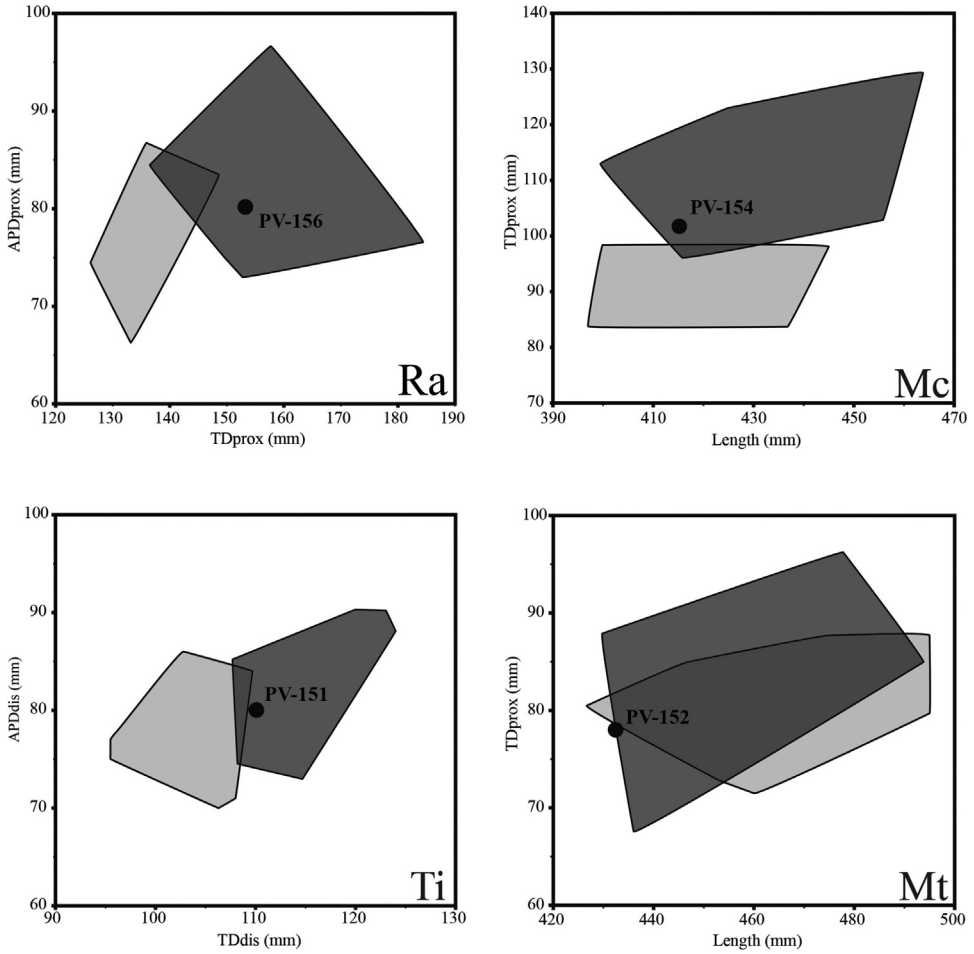

Fig. 3. Dispersion plots showing the relative size of limb bones of *Helladotherium duvernoyi* from Kavakdere. The light grey areas represent the *Samotherium major* morphospaces. The dark grey areas represent the *Helladotherium duvernoyi* morphospaces. Circle points represent the Kavakdere specimens. Hu: humerus; Mc: metacarpus; Ti: tibia; Mt: metatarsus; TD: transverse diameter; APD: antero-posterior diameter; prox: proximal; dis: distal. All measurements given in millimetres (data from Bohlin, 1926; Geraads, 1994; Iliopoulos, 2003; Kostopoulos, 2009; personal data of AX).

Fig. 3. Diagramme des relevés montrant la taille relative des os des membres d'*Helladotherium duvernoyi* de Kavakdere. Les zones en gris clair représentent les morpho-espaces de *Samotherium major*, les zones en gris foncé ceux d'*Helladotherium duvernoyi*. Les cercles noirs représentent les échantillons de Kavakdere. HU : humérus ; Mc : métacarpien ; Mt : métatarsien ; TD ; diamètre transversal ; APD : diamètre antéro-postérieur ; prox : proximal ; dis : distal. Toutes les mesures sont en millimètres (données d'après Bohlin, 1926 ; Geraads, 1994 ; Iliopoulos, 2003 ; Kostopoulos, 2009 ; données personnelles de AX).

Comparisons and remarks: *Helladotherium duvernoyi* constitutes one of the most common large-sized Miocene giraffids. The stratigraphic origin of the earliest collection from the type locality of Pikermi, described by Gaudry (1860), is unknown. Therefore, there is no designated holotype. However, all the sivatheres of the type locality belong to the same species, and therefore, the assignment of a lectotype is unnecessary (Geraads et al., 2005). *Helladotherium duvernoyi* is the only species assigned to the genus and it appears in several localities of the Greco-Iranian province, from MN9 to MN13 (Athanassiou, 2002; Bonis et al., 1992; Iliopoulos, 2003; Kostopoulos, 2009; Kostopoulos and Koufos, 2006; Kostopoulos and Saraç, 2005; Kostopoulos et al., 1996, 2003, 2009; Koufos, 1990, 2006; Koufos et al., 2009; Marinos and Symeonidis, 1974; Solounias, 1981a, 1981b).

Although in the studied collection dental remains of *H. duvernoyi* are completely absent, a collection of fore and hind-limb specimens can clearly distinct this taxon from other large Miocene giraffids, such as *Samotherium* Forsyth-Major (1888) and *Bramatherium* Falconer (1845). Morphological differences of post-cranial elements of *H. duvernoyi*, *Samotherium boissieri*, *S. major* and *Bramatherium megacephalum* were given by Kostopoulos (2009), Rios et al. (2016), and Solounias and Danowitz (2016a).

Due to the scarcity of the fossil material, there is no obvious sexual dimorphism detected within *Helladotherium* from Kavakdere. However, metrical comparison with specimens from other fossiliferous sites reveal the relative size of the large sivathere from Kavakdere. Following Roussiakis and Iliopoulos (2004), we compared ratios between the proximal and distal epiphyses of all post-cranial long bones (radius, metacarpus, tibia and metatarsus), from various fossiliferous localities, where the size variation is more prominent (Fig. 3). In all cases, the Kavakdere specimens

plot very close to the morphospaces of *Samotherium major*, suggesting a relatively small size of *H. duvernoyi*.

Genus *Bramatherium* Falconer, 1845
Bramatherium perimense (Falconer, 1845)

Material: PV-150, left metatarsal; PV-153, left metatarsal; PV-236, proximal phalanx (Fig. 4; Table 2).

Descriptions: The fossil material of *B. perimense* is limited to two metatarsals, as well as a proximal phalanx. The metatarsus (PV-150, PV-153; Fig. 4A-B) is very long and robust. Proximally, the surface for the naviculocuboideum is oval to kidney-shaped since the palmar rim of the surface bends notably towards the synovial fossa. The surface for the external cuneiform is long and slightly larger than the surface for the naviculocuboideum, with an almost rectangle semi-circular shape. The surface for the medial cuneiform is small, with the palmar rim being slightly bifurcated. Between these two surfaces, an additional small triangle-shaped articular surface can be noted. This surface is on the same level as the cuneiform surfaces and represents the remnant of the lateral fifth metatarsal. In plantar view, the epicondyles are all strong and well-separated. The dorsal head of the lateral epicondyle is rounded, bearing a small bony protuberance proximally. The ventral head of the lateral epicondyle is long and thin, leading to the lateral ridge of the central trough. The medial epicondyle is generally stronger and more robust. The ventral head is blunt but very strong, leading to the blunt medial ridge of the central trough. Between the medial and lateral epicondyles there is a weak but visible spindle-shaped pygmaios, which is slightly elevating above the surface of the basis. The central trough is somewhat shallow, and it flattens towards the distal shaft. On the distal epiphysis, the keels of the medial and the lateral condyles are strong and equally developed in plantar and dorsal aspect.

The proximal phalanx (PV-236; Fig. 4C) is very long and robust. The medial and lateral margins of the corpus are only slightly concave. On the articular fovea, a deep trough is separating the medial from the larger lateral articular facet. The palmar tubercles are long, covering approximately the upper 40% of the phalanx. The head is strongly asymmetrical and has almost the same width as the corpus.

Comparisons and remarks: *Bramatherium*, including the synonymous genera *Hydaspitherium* Lydekker (1876) and *Vishnutherium* Lydekker (1876), constitutes a widespread upper Miocene sivatherine. The taxon has been reported from numerous Asian localities in Thailand, Myanmar, India, Pakistan, United Arab Emirates and Turkey (Antoine et al., 2013; Bhatti et al., 2012; Bibi et al., 2013; Brunet et al., 1981; Colbert, 1935; Gaur et al., 1985; Gentry, 2003; Geraads and Güleç, 1999; Khan et al., 2014; Lewis, 1939; Lydekker, 1878; Matthew, 1929; Nishioka et al., 2014; Raza et al., 2002; Sehgal, 2015; Sehgal and Nanda, 2002a, 2002b; Welcomme et al., 1997). However, the determination of the taxon has been almost solely based on cranial and dental characters, while post cranial elements are rarely described.

Bramatherium is no stranger to the fossiliferous horizons at Kavakdere, since it was the first taxon to be comprehensively described from the locality (Geraads and Güleç, 1999). The authors of this study also included a brief description of a humerus and a metatarsus. Later, new comparative studies focused on metatarsals and astragali, gave a better image and understanding of the osteology of the taxon (Rios et al., 2016; Solounias and Danowitz, 2016a), especially in comparison to *H. duvernoyi*, since the two taxa have been considered synonymous in the past (Matthew, 1929). Nevertheless, the osteological differences between most post cranial skeletal elements of the different *Bramatherium* species are still unclear.

The three species recognized are *B. perimense*, *B. megacephalum* Lydekker (1876), and *B. grande* Lydekker (1876), with the latter circumscription based solely on dental material. The post cranial long bones, and especially the metapodials of *Helladotherium* and *Bramatherium* exhibit a high metrical overlapping (Solounias, 2007; Fig. 5). Therefore, metrical comparison alone, cannot provide a conclusive taxonomic interpretation. Nevertheless, metatarsals of *H. duvernoyi* and *B. megacephalum* differ in many ways, with *B. megacephalum* having an additional distinct pygmaios, as well as a remainder of the lateral fifth metapodial, which are absent in *H. duvernoyi* (Rios et al., 2016).

The above-described metatarsals both exhibit the general sivatherine characters. However, both PV-150 and PV-153 have a small but distinct pygmaios as well as a remnant of the lateral fifth metatarsal. A metatarsal of *Bramatherium* sp. from Thailand (RIN 794; Nishioka et al., 2014: Fig. 4) demonstrates all the above-mentioned characters, but the pygmaios is notably more prominent than in the Kavakdere specimens, putting RIN 794 closer to *B. megacephalum* (AMNH 19688; Rios et al., 2016: Fig. 8). In addition, the irregularly shaped surface for the medial cuneiform in the Kavakdere metatarsalia, as opposed to the perfectly rounded surface of *H. duvernoyi*, fits closer to the almost heart-shaped medial cuneiform surface of *B. megacephalum* (Rios et al., 2016). This surface is not visible in the Thai (RIN 794) specimens due to the attachment of the naviculocuboideum at the basis of the metatarsal. Metrically, PV-150 comprises the longest *Bramatherium* metatarsal ever recorded. It appears approximately 10% longer and 14% and 20% wider in the anteroposterior diameters of the proximal and distal epiphysis, respectively, than in PV-153. This size difference could be attributed to sexual dimorphism, as noticed in long post cranial bones of *Helladotherium duvernoyi* and *Bohlinia attica*, Gaudry and Lartet (1856) (Roussiakis and Iliopoulos, 2004). *Bramatherium* shows a wide metatarsal length fluctuation (Fig. 6A). On a species level though, it becomes clear that *B. perimense* is generally larger than *B. megacephalum* (Fig. 6B), which can also be observed in dental measurements (Lewis, 1939).

First phalanges of *Bramatherium* are reported and illustrated by Colbert (1935) and they share the general sivatherine characters, such as a very long and thick corpus and strong palmar tubercles (Kostopoulos, 2009). The Kavakdere specimen also possesses these characters. However, the fact that PV-236 is much bigger than the rest of the recovered sivatherine phalanges, and it has a notably longer and more robust palmar tubercles than

Fig. 4. Fossil post-cranial material of *Bramatherium perimense* from Kavakdere. A: PV-150, left metatarsal, (i) dorsal and (ii) plantar aspect; B: PV-153, left metatarsal, (i) dorsal and (ii) plantar aspect; C: PV-236, first phalanx, (i) dorsal and (ii) lateral aspect. The scale equals 20 centimetres.
Fig. 4. Matériel post-crânien fossile *Bramatherium perimense* de Kavakdere. A : PV-150, métatarsien gauche, aspects dorsal (i) et plantaire (ii) ; B : PV-153, métatarsien gauche, aspects dorsal (i) et plantaire (ii) ; c : PV-236, première phalange, aspects dorsal (i) et lateral (ii). Échelle = 20 cm.

Table 2
Measurements of post-cranial elements of *Bramatherium perimense* from Kavakdere. Sin: left; Dex: right; L: length; APD: antero-posterior diameter; TD: transverse diameter; prox: proximal; dia: diaphysis; dis: distal. All measurements given in millimetres.
Tableau 2
Mesures des éléments post-crâniens de *Bramatherium perimense* de Kavakdere. Sin : gauche ; Dex : droite ; L : longueur ; APD : diamètre antéro-postérieur ; TD : diamètre transversal ; prox : proximal ; dia : diaphysis ; dis : distal. Toutes les mesures sont en millimètres.

Metatarsus

Inv. Number	Taxon	Sin/Dex	L	TDprox	APDprox	TDdia	APDdia	TDdis	APDdis
PV-150	*Bramatherium perimense*	sin	486.9	93.76	94.9	56.85	61.03	100.8	60.15
PV-153	*Bramatherium perimense*	sin	442.83	85.67	83.04	49.04	50.12	86.19	55.76

Phalanx 1

Inv. Number	Taxon	L	TDprox	APDprox	TDdis	APDdis
PV-236	*Bramatherium perimense*	123.54	54.89	61.79	53.14	40.04

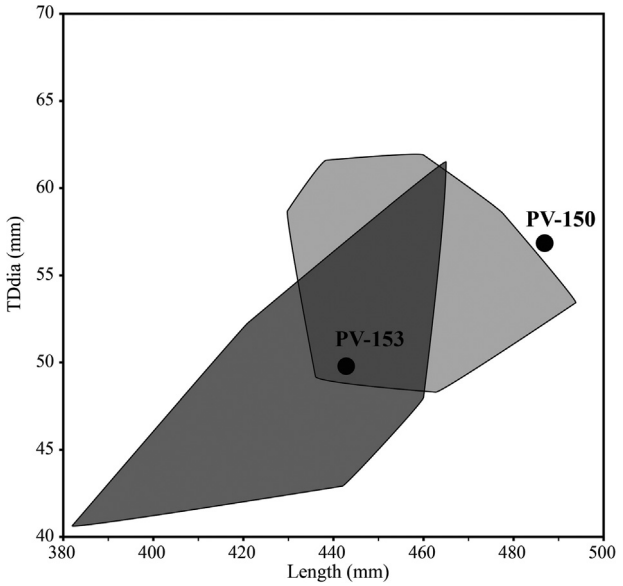

Fig. 5. Scatter diagram of the total length versus the transverse diameter of the diaphysis of the metatarsals of *Bramatherium perimense* from Kavakdere (dark points). Light grey area represents the morphospace of *Helladotherium*. Dark grey area represents the morphospace of *Bramatherium*. The measurements are given in millimetres (data from Iliopoulos, 2003; Kostopoulos, 2009; Nishioka et al., 2014; Rios et al., 2016; personal data of AX).
Fig. 5. Diagramme de dispersion de la longueur totale en fonction du diamètre transversal de la diaphyse des métatarsiens de *Bramatherium perimense* de Kavakdere (points noirs). La zone en gris clair représente le morpho-espace d'*Helladotherium*, la zone en gris foncé celui de *Bramatherium*. Les mesures sont fournies en millimètres (données d'Iliopoulos, 2003 ; Nishioka et al., 2014 ; Rios et al., 2016 ; données personnelles de AX).

in *H. duvernoyi*, suggest that it belongs to the larger *B. perimense* instead of the smaller *H. duvernoyi*.

Subfamily Palaeotraginae Pilgrim, 1911
Genus Palaeotragus Gaudry, 1861
Palaeotragus rouenii (Gaudry, 1861)

Material: PV-176, right mandible with d3-m1; PV-244, left naviculocuboideum; PV-226, proximal phalanx (Fig. 7; Table 3).

Descriptions: Dental elements of *P. rouenii* from Kavakdere are only represented by a mandible bearing deciduous dentition (PV-176; Fig. 7A). The clade is short and thin, and the second deciduous premolar is broken. The d3 is long and strongly molarized. The anterior conid and anterior stylid are big and almost equally developed, with the latter being slightly stronger. The anterolabial cristid is large, projecting antero-labially, creating a small crescent surface, in occlusal aspect. The mesolingual and mesolabial conids are the largest cusps and they are well-separated by a transverse fossa. The mesolingual conid carries a strong fold, which is projecting postero-lingually, within the fossa. The posterolabial and posterolingual conids are isolated and separated from each other by a very thin and long fossa with a posterolingual direction. Both conids are strongly developed. Cingula and stylids are completely absent.

The d4 is long with very well-defined ectostylids. All lobes are simple, getting gradually larger posteriorly. The anterolabial conid is thin, with its apex being pointy labially. The anterior stylid is small and curved labially, being in contact with the base of the posterolabial conid of the d3. The anterolingual conid is simple and it extends posteriorly with a strong external-postmetacristid-like

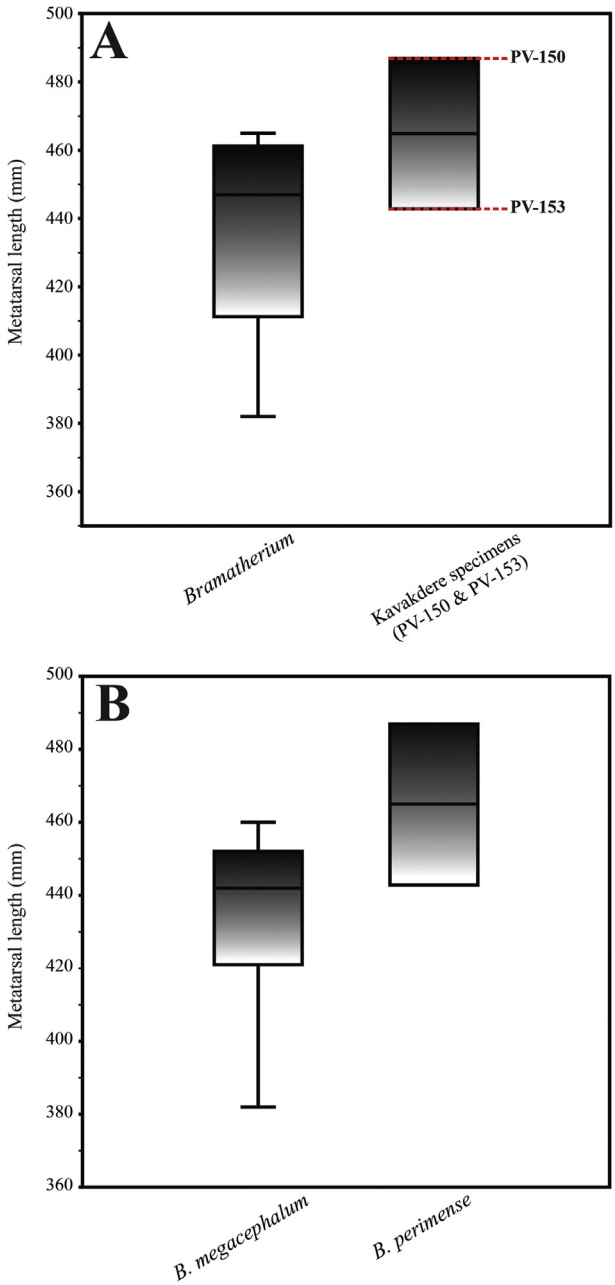

Fig. 6. Box plot of metatarsal length of *Bramatherium*. A. Relative size of *Bramatherium perimense* from Kavakdere in comparison with the metatarsal length of *Bramatherium* individuals from various localities. B. Relative metatarsal length *of Bramatherium megacephalum* and *Bramatherium perimense*. Each box represents 50% of the range of the premolar length, while the top and the bottom bars represent the overall range of the length. The horizontal line in the centre of each box represents the median of the sample (data from Iliopoulos, 2003; Kostopoulos, 2009; Nishioka et al., 2014; Rios et al., 2016; personal data of AX).

Fig. 6. *Box plot* de la longueur du métatarsien de *Bramatherium*. A. Taille relative de *Bramatherium perimense* de Kavakdere comparée à la longueur du métatarsien d'individus de *Bramatherium* de localités variées. B. Longueur relative du métatarsien de *Bramatherium megacephalum* et de *Bramatherium perimense*. Chaque boîte représente 50 % de la gamme de longueur de la prémolaire, tandis que les barres au sommet et à la base représentent le total de la longueur. La ligne horizontale au centre de chaque boîte représente la médiane de l'échantillonnage (données de Iliopoulos, 2003 ; Kostopoulos, 2009 ; Nishioka et al., 2014 ; Rios et al., 2016 ; données personnelles de AX).

enamel projection, which surrounds the mesostylid completely. The metaconid and protoconid are both strong and simple and the metastylid is small and blunt. The entoconid is large, getting sturdier towards the base of the crown. The entostylid is small and isolated. The hypoconid is also large and the posterior apex of the post-hypocristid is bifurcated, surrounding the isolated entostylid.

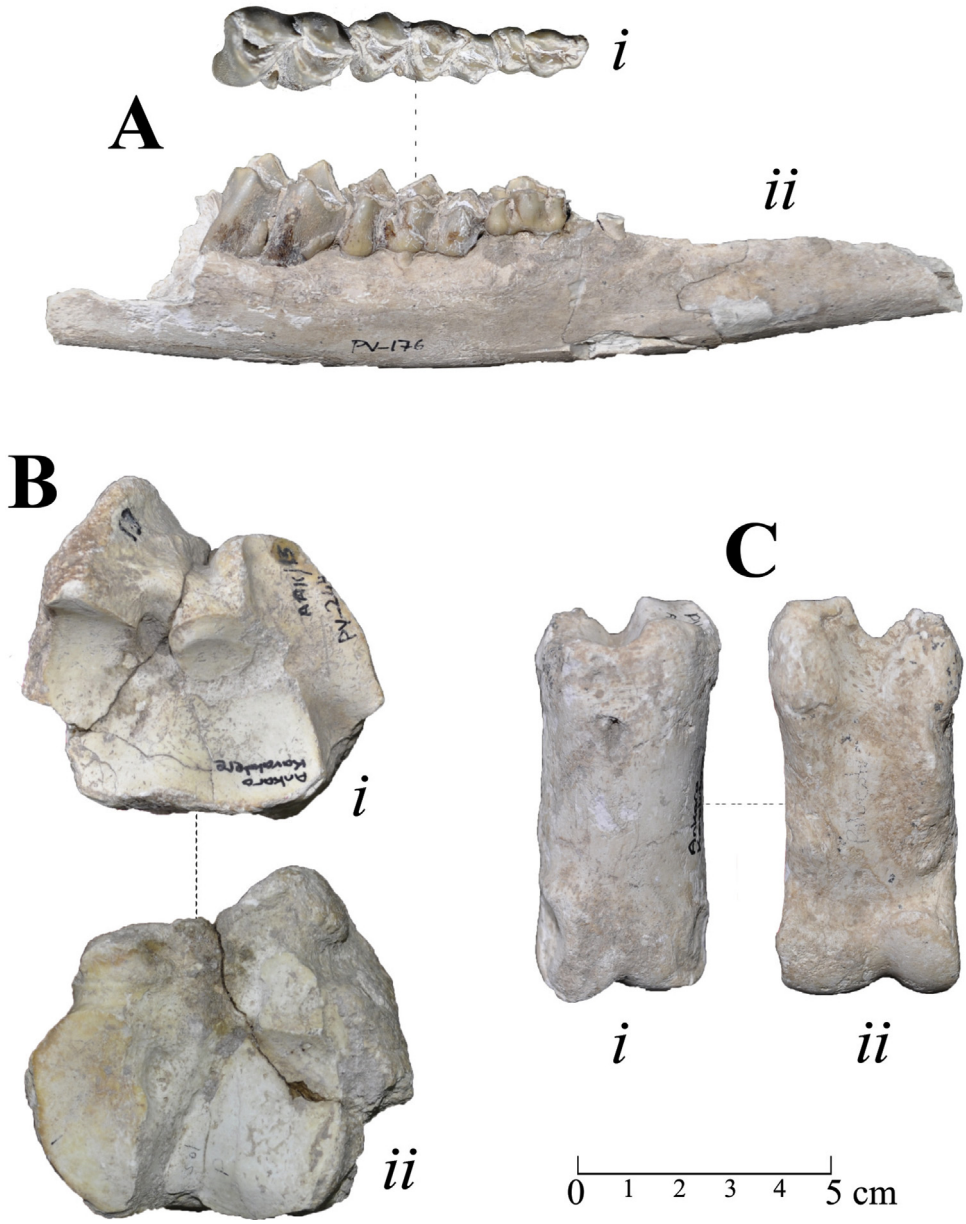

Fig. 7. Fossil dental and post-cranial material of *Palaeotragus rouenii* from Kavakdere. A: PV-176, right mandible with d3-m1, (i) occlusal and (ii) labial view; B: PV-244, left naviculocuboideum, (i) proximal and (ii) distal view; C: PV-226, first phalanx (i) dorsal and (ii) palmar view. The scale equals 5 cm.
Fig. 7. Matériel dentaire et post-crânien fossile de *Palaeotragus rouenni* de Kavakdere. A : PV-176, mandibule droite avec d3-m1 en vues occlusale (i) et labiale (ii). B : PV-244, naviculocoboideum en vues proximale (i) et distale (ii). C : PV-226, première phalange en vues dorsale (i) et palmaire (ii). Échelle = 5 cm.

The m1 carries a very strong anterior cingulum, forming a small stylid towards the protocone, as well as a tall and sharp ectostylid. In occlusal aspect, the overall morphology of the m1 is simple. The anterior lobe is slightly larger than the posterior lobe, due to the strong lingual projection of the metaconid. The anterior and posterior fossae are narrow and deep, while the labial conids exhibit no folds.

The naviculocuboideum (PV-244; Fig. 7B) has a subrectangle shape, proximally. The astragalar facets are parallel and almost equal in size. The calcaneal facet is very wide, long and it is not extending behind the lateral peak. In distal view, the facet for the metatarsal is small and semicircular. The facet for the external cuneiform is larger than the metatarsal facet, having a more rectangular shape. The facet for the medial cuneiform is small, triangular and well separated from the external cuneiform facet by a blunt crest.

The proximal phalanx (PV-226; Fig. 7C) is thin and long. The medial and lateral margins of the body are parallel to each other. The medial and lateral articular facets on the fovea are well separated by a deep and wide trough. In lateral aspect, the palmar tubercle is well-developed, but

Table 3
Measurements of dental and post-cranial elements of *Palaeotragus rouenii* from Kavakdere. Sin: left; Dex: right; hp: height of the mandible in front of P2; L: length; I: width; d3: lower third deciduous premolar; d4: lower fourth deciduous premolar; m1: lower first molar; APD: antero-posterior diameter; TD: transverse diameter; prox: proximal; dis: distal; med: medial; Hmax: maximum height; H1: Height of the cubonavicular on the level of the medial astragalar surface; H2: Height of the cubonavicular on the level of the lateral astragalar surface. All measurements given in millimetres.
Tableau 3
Mesures des éléments post-crâniens et dentaires de *Paélaeotragus rouenii* de Kavakdere. Sin : gauche ; Dex : droite ; hp : hauteur de la mandibule en avant de P2 ; L : longueur l : largeur ; d3 : troisième pré-molaire inférieure caduque ; d4 : quatrième prémolaire inférieure caduque ; m1 : première molaire inférieure ; APD diamètre antéro-postérieur ; TD : diamètre transversal ; prox : proximal ; dis : distal ; med : médial : Hmax : hauteur maximum ; H1 : hauteur du cubonaviculaire au niveau de la surface médiale de l'astragale ; H2 : hauteur du cubonaviculaire au niveau de la surface latérale de l'astragale. Toutes les mesures sont en millimètres.

Lower deciduous dentition

Inv. Number	Taxon	Sin/Dex	hp	Ld3	Id3	Ld4	Id4	Lm1	lm1
PV-176	*Palaeotragus rouenii*	dex	26.13	17.72	9.22	27.13	13.98	24.06	15.74

Naviculocuboideum

Inv. Number	Taxon	Sin/Dex	TD	APDmed	APDmax	Hmax	H1	H2
PV-244	*Palaeotragus rouenii*	sin	71.52	53.58	64.11	45.93	18.73	28.88

Phalanx 1

Inv. Number	Taxon	L	TDprox	APDprox	TDdis	APDdis
PV-226	*Palaeotragus rouenii*	78.92	34.28	37.42	33.93	25.54

limited on the proximal part of the phalanx. The medial palmar tubercle is less developed than the lateral one, but it extends distally, stopping right above the distal trochlea.

Comparisons and remarks: *Palaeotragus* constitutes the most abundant late Miocene giraffid in the Greco-Iranian province (Gentry and Heizmann, 1996). The plethora or dental and post-cranial fossil elements brought to light, separated the *Palaeotragus* taxa into two distinct size groups: a small-sized group including *P. rouenii* and *Palaeotragus microdon* Koken (1885) and a large-sized group including *Palaeotragus coelophrys* Rodler and Weithofer (1890) and *Palaeotragus quadricornis* Bohlin (1926) (Geraads, 1986; Iliopoulos, 2003; Kostopoulos, 2009; Kostopoulos and Saraç, 2005; Kostopoulos et al., 1996).

Palaeotragus rouenii comprises the most common palaeotragine species and was originally described from Pikermi, Greece (Gentry and Heizmann, 1996). However, despite the large number of findings, deciduous dentition of *Palaeotragus* is scarce, with only a few specimens mentioned from China, Ukraine, Moldova, Bulgaria, and Greece, and in most cases with pictures or illustrations lacking (Bakalov et al., 1962; Bohlin, 1926; Borissiak, 1914; Godina, 1979). Metrical comparison of the lower deciduous dentition of *P. coelophrys* from China and Ukraine and *P. rouenii* from Moldova and Greece, reveals a large metrical variation on the length of d3 and d4 (Fig. 8). In both teeth, the large overlapping between the two taxa is significant. Even though the available data is limited, it is evident that the length of the deciduous premolars falls within the variation of *P. coelophrys*, while the length/width ratio of the d3 of PV-176 shows a closer resemblance to *P. rouenii*.

The lack of thorough descriptions and illustrations of deciduous lower dentition of *Palaeotragus* in previous studies, limits a morphological variation study. A mandible of *Palaeotragus* cf. *coelophrys* from China (Ex. 9; Bohlin, 1926: Plate II), as well as a mandible of *P. rouenii* from Samos (SMNS 13281e), share some common characters with PV-176. SMNS 13281e represents a part of left mandible with the d3, d4 and the proximal lobe of the m1 preserved. Although this specimen is notably more worn than *P. rouenii* from Kavakdere, SMNS 13281e demonstrates an almost identical morphology with PV-176. More specifically, on the d3, both specimens share a strong and crescent-shaped anterolabial cristid, the large and well-separated mesolingual and mesolabial conids and the well separated posterolabial and posterolingual conids. On the d4 of both individuals, the anterolingual conid exhibits a strong external-postmetacristid-like enamel protuberance, which is better pronounced in the Kavakdere specimen. Lastly, both specimens disclose an isolated entostylid. In contrast, the Chinese specimen (Ex. 9) demonstrates an isolated anterior conid and a much more developed anterior stylid and anterolabial cristid. Additionally, the posterolingual conid is strongly connected to the mesolingual conid.

Postcranial elements of late Miocene giraffids are commonly infrequent (Kostopoulos, 2009). Withal, naviculocuboideum specimens are also scarce. However, the metrics reveal that PV-244 belongs to a small palaeotragine. Measurements from previous studies show that *Samotherium boissieri* appears to be always larger than *P. rouenii* (Fig. 9). The transverse diameter (TD) of PV-244 is 71.52, slightly smaller than the mean value of the transverse diameter of *S. boissieri* from Samos (Kostopoulos, 2009). Conclusively, based on the above-listed descriptions and the further on comparisons, we assign the above-mentioned specimens to *P. rouenii*.

Genus *Samotherium* Forsyth-Major, 1888
Samotherium boissieri (Forsyth-Major, 1888)

Material: PV-242, right calcaneus; PV-243, right astragalus (Fig. 10 ; Table 4).

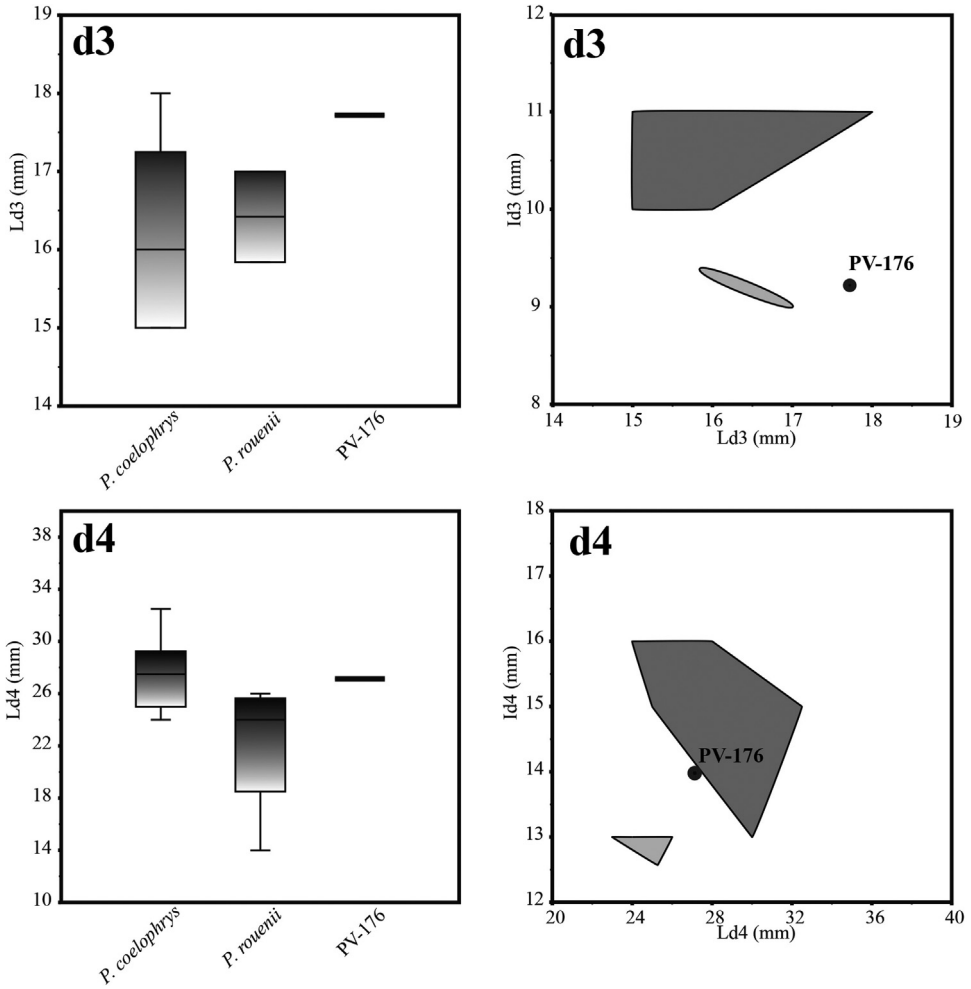

Fig. 8. Box plots and scatter plots exhibiting the relative size of the deciduous dentition of *Palaeotragus rouenii* and *Palaeotragus coelophrys*. The light grey areas represent the morphospaces of *Palaeotragus rouenii*. The dark grey areas represent the morphospaces of *Palaeotragus coelophrys*. Circle points represent the Kavakdere specimens. Each box represents 50% of the range of the premolar length. The top and the bottom bars represent the overall range of the length. Horizontal line in the centre of each box represents the median of the sample. Measurement given in millimetres (data from Bohlin, 1926; Bakalov et al., 1962; Godina, 1979; personal data of AX).

Fig. 8. *Box plots* et nuage de points montrant la taille relative de la dentition caduque de *Palaeotragus rouenni* et *Palaeothragus coelophrys*. Les zones en gris clair représentent les morpho-espaces de *Palaeotragus rouenni*, et les zones en gris foncé ceux de *Palaeotragus coelophrys*. Les points noirs représentent les spécimens de Kavakdere. Chaque boîte représente 50 % de la gamme de longueur de la prémolaire. Les barres au sommet et à la base représentent le total de la longueur. La ligne horizontale au centre de chaque boîte représente la médiane de l'échantillonnage. Les mesures sont fournies en millimètres (données de Bohlin, 1926 ; Bakalov et al., 1962 ; Godina, 1979 ; et données personnelles de AX).

Table 4
Measurements of post-cranial elements of *Samotherium boissieri* from Kavakdere. Sin: left; Dex: right; L: length; APD: antero-posterior diameter; TD: transverse diameter; prox: proximal; dis: distal; lat: lateral; med: medial; Hmax: maximum height; Hmin: distance between the sustentaculum tali and the tuber calcanei; tuber: tuber calcanei. All measurements given in millimetres.

Tableau 4
Mesures de éléments post-crâniens de *Samotherium boissieri* de Kavakdere. Sin : gauche ; Dex : droite ; L : longueur ; APD : diamètre antéro-postérieur ; TD : diamètre transversal ; prox : proximal ; dis : distal ; lat : latéral : med : médial ; Hmax : hauteur maximum ; Hmin : distance entre le sustentaculum tali et le tuber calcanei ; tuber : tuber calcanei. Toutes les mesures sont en millimètres.

Astragalus

Inv. Number	Taxon	Sin/Dex	Llat	Lmed	TDprox	TDdis
PV-243	*Samotherium boissieri*	dex	88.1	80.95	58.07	56.16

Calcaneus

Inv. Number	Taxon	Sin/Dex	Hmax	Hmin	TDmax	APDmax	TDtuber	APDtuber
PV-242	*Samotherium boissieri*	dex	156.68	105.34	49.69	66.21	38.99	45.62

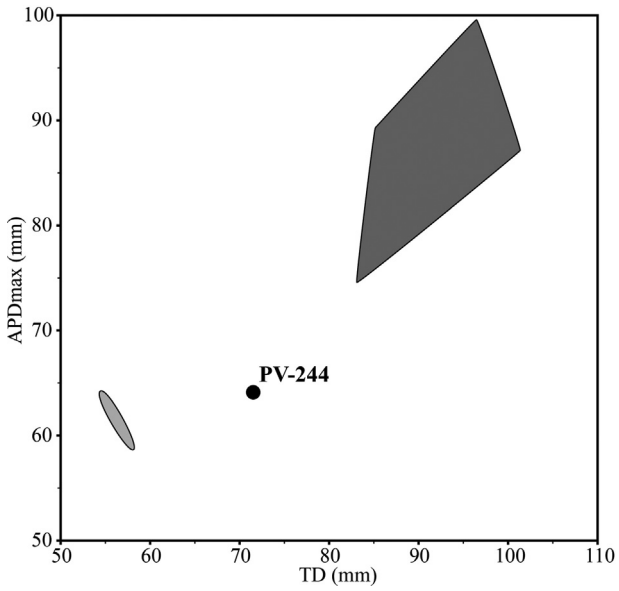

Fig. 9. Bivariate plot of the transverse diameter versus the maximum antero-posterior diameter of the naviculocuboideum of *Palaeotragus rouenii*. The circle point represents the Kavakdere specimen. The light grey areas represent the morphospaces of *Palaeotragus rouenii*. The dark grey areas represent the morphospaces of *Samotherium boissieri*. The measurements are given in millimetres (data from Kostopoulos, 2009; personal data of AX).
Fig. 9. Représentation bivariée du diamètre transversal en fonction du diamètre antéro-postérieur maximum du naviculocuboideum de *Palaeotragus rouenni*. Le pont noir représente le spécimen de Kavakdere. Les zones en gris clair représentent les morpho-espaces de *Palaeotragus rouenni* et les zones en gris foncé ceux de *Samotherium boissieri*. Les mesures sont fournies en millimètres (données de Kostopoulos, 2009 ; données personnelles de AX).

Descriptions: PV-242 represents a complete calcaneum (Fig. 10A). The sustentaculum tali is fairly developed and equally developed laterally and medially. The groove for the tendon of M. flexor digitorum lateralis is deep and well defined. The articular surface for the lateral malleolus is strong and robust. The articular surface for the cubonavicular is slightly concave, with parallel margins.

The astragalus (PV-243; Fig. 10B) is almost symmetrical in dorsal aspect. The lateral ridge of the trochlea is only slightly larger than the medial one. The trochlear groove is wide, and the central fossa is shallow. The head is also symmetrical, with the lateral trochlea being somewhat bigger than the medial trochlea. In ventral view, the proximal triangular fossa is deep, extending into an equally deep interarticular groove. The medial and lateral ridges of the ventral articular surface are parallel. There is a notable medial scala. The distal intracephalic fossa appears in two distinct areas, both positioned laterally, with the second one placed more distally.

Comparisons and remarks: *Samotherium* was first described by Forsyth-Major (1888) based on the remains of a large artiodactyle from Samos, but without a designated holotype. The two most common *Samotherium* species, which were widespread across the Pikermian biome, are *S. boissieri* and the larger *S. major*. *Samotherium major* is a descendant of *S. boissieri* and replaced the latter about 7.4 million years ago, at the transition between the MN11 and MN12 zones (Kostopoulos, 2009; Kostopoulos et al., 2003). *S. boissieri* is reported from numerous localities in Greece, Turkey, and Iraq (Becker-Platen et al., 1975; Geraads, 1974; Köhler et al., 1995; Kostopoulos, 2009 and literature within; Solounias and Danowitz, 2016b; Thomas et al., 1980). In Anatolia, *S. boissieri* was found at Gülpınar, Mahmutgazi, Kemiklitepe A/B, Akkaşdağı and Taşkinpaşa (Becker-Platen et al., 1975; Geraads, 1994; Karadenizli et al., 2005; Kostopoulos and Saraç, 2005; Saraç, 2003; Şenyürek, 1954).

The overall structure of the two above-described specimens from Kavakdere agree with the morphology of a medium-sized palaeotragine (Kostopoulos, 2009; Solounias and Danowitz, 2016a). Further metrical comparison of PV-242 and PV-243 with *S. boissieri* and *S. major* from various fossiliferous sites agrees with the morphological conclusion (Fig. 11). Specifically, the calcaneus from Kavakdere shows a small maximum height, plotting very close to the small *S. boissieri* individuals from Samos. The astragalus falls almost in the middle of the morphospaces of *S. boissieri*. With a lateral astragalar trochlear length (Llat) of 88.1 mm, in addition to the small maximum calcaneal length, it is concluded that *S. boissieri* is represented in Kavakdere by one female individual (Kostopoulos, 2009).

Genus *Alcicephalus* Rodler and Weithofer, 1890
Alcicephalus neumayri (Rodler and Weithofer, 1890)

Material: PV-245, right trapezoideo-capitatum; PV-235, right astragalus; PV-238, right naviculocuboideum (Fig. 12; Table 5).

Reference material: NHMW 2019/0018/0001, left astragalus; NHMW 2019/0018/0002, left astragalus; NHMW 2019/0018/0003, left astragalus; NHMW 2019/0018/0004, right astragalus (Table 6).

Descriptions: The trapezoideo-capitatum (PV-245; Fig. 12A) has a sub-quadrangular shape in cranial aspect, with the transverse diameter being slightly larger than

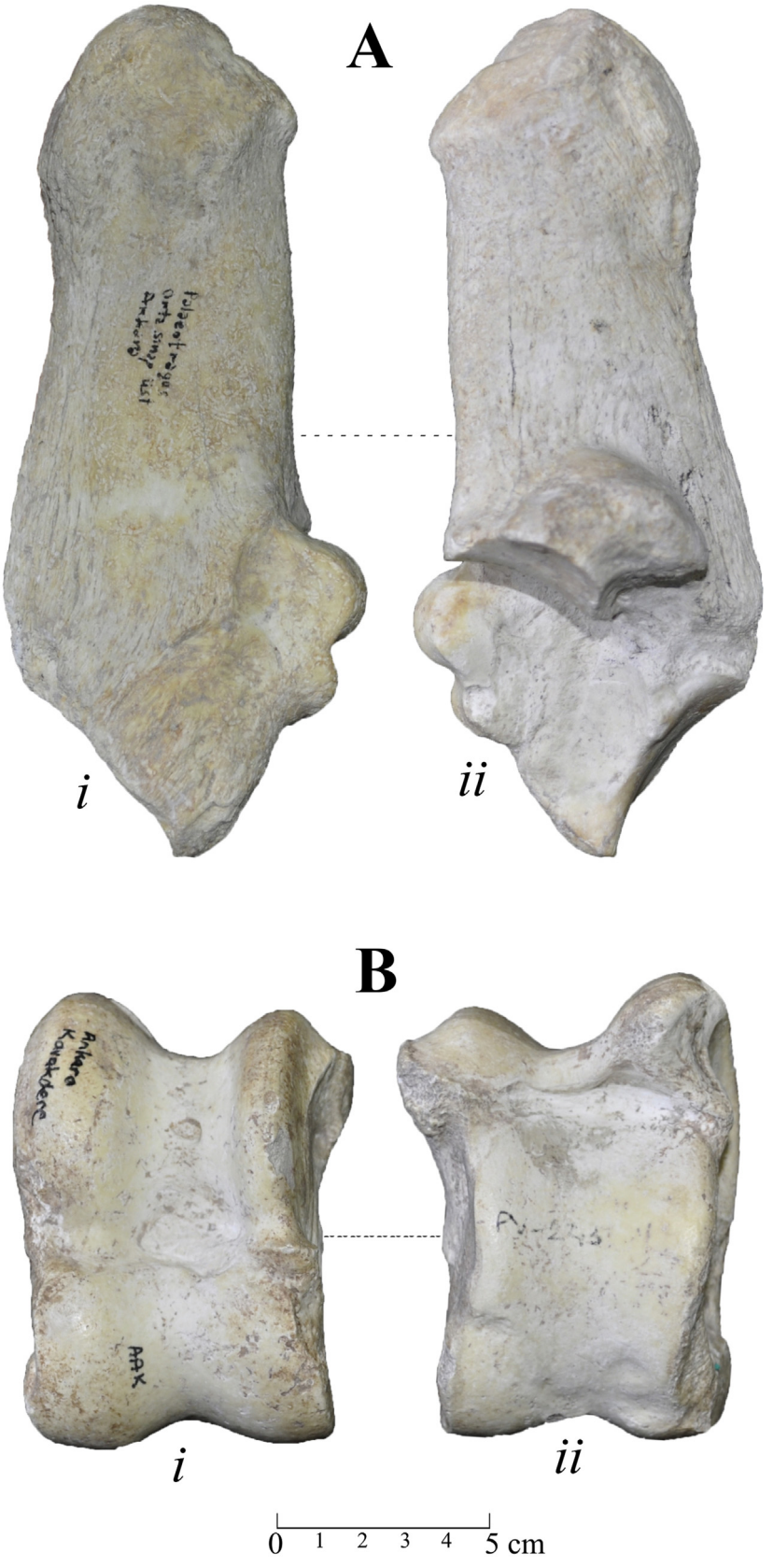
A
i
ii
B
i
ii
0 1 2 3 4 5 cm

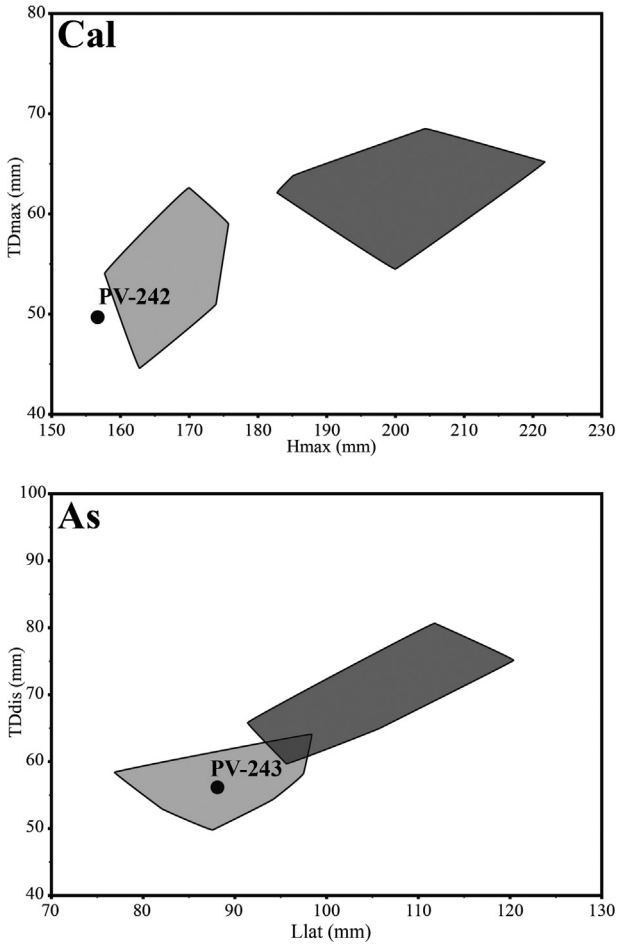

Fig. 11. Bivariate plots for the calcaneus and astragalus of *Samotherium boissieri* from Kavakdere (circle points). The light-grey-highlighted areas represent the morphospaces of *Samotherium boissieri*. The dark grey areas represent the morphospaces of *Samotherium major*. Cal: calcaneus; As: astragalus; Hmax: maximum height of the calcaneus; TDmax: maximum transverse diameter on the level of the sustentaculum tali; Llat: length of the lateral trochlea of the astragalus; TDdist: transverse diameter of the distal head of the astragalus. The measurements are given in millimetres (data from Iliopoulos, 2003; Kostopoulos, 2009; personal data of AX).

Fig. 11. Représentation bivariée pour le calcanéum et l'astragale de *Samotherium boissieri* de Kavakdere (points noirs). Les zones en gris clair représentent les morpho-espaces de *Samotherium boissieri* et les zones en gris foncé ceux de *Samotherium major*. Cal : calcanéum ; As : astragale ; Hmax : hauteur maximum du calcanéum ; TDmax : diamètre transversal maximum au niveau du sustentaculum tali ; Llat : longueur de la trochlée latérale de l'astragale. TDdist : diamètre transversal de la tête distale de l'astragale. Les mesures sont fournies en millimètres (données d'Iliopoulos, 2003 ; Kostopoulos, 2009 ; données personnelles de AX).

the antero-posterior diameter (Table 5). The medial wall is straight, and the medial groove is shallow and wide. The articular surface for the scaphoid is deep and the lunatum surface is highly asymmetrical and shallow. The crests separating the two facets are strong but short and blunt.

There is only one astragalus of *A. neumayri* found (PV-235; Fig. 12B). In dorsal aspect, the lateral ridge of the trochlea is significantly taller and only slightly thicker than the medial ridge. However, both ridges are straight and parallel to each other. The central fossa is wide and shallow, extending laterally with a small grove towards the lateral collum tali. The lateral collum tali is flat, while the medial collum tali carries a pointy bulge. In ventral view, the interarticular groove is narrow, leading to a wider triangular fossa. The ventral articular surface is irregularly shaped, with the medial ridge carrying a weak medial scala, which is visible on the medial ridge but not there are no defined limits on the ventral articular surface. The lateral margin gets notably concave distally. The distal intracephalic fossa is present but faint and not well confined.

Fig. 10. Fossil post-cranial material of *Samotherium boissieri* from Kavakdere. A: PV-242, right calcaneus (i) lateral and (ii) medial view; B: PV-243, right astragalus, (i) dorsal and (ii) plantar view. The scale equals 5 cm.

Fig. 10. Matériel post-crânien fossile de *Samotherium boissieri* de Kavakdere. A : PV-242, calcanéum droit en vues latérale (i) et médiale (ii). B : PV-243, astragale droit en vues dorsale (i) et plantaire (ii). Échelle = 5 cm.

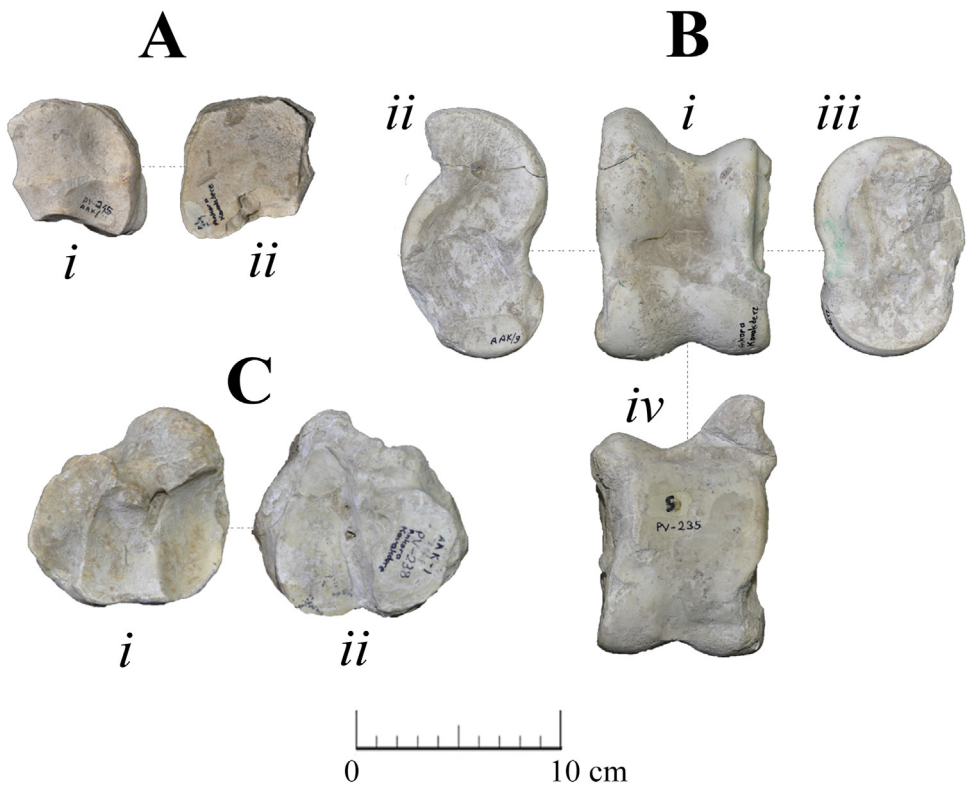

Fig. 12. Fossil post-cranial elements of *Alcicephalus neumayri* from Kavakdere: A: PV-245, right trapezoideo-capitatum, (i) proximal and (ii) distal view; B: PV-235, right astragalus, (i) dorsal and (ii) lateral view, (iii) medial view and (iv) plantar view; C: PV-238, right naviculocuboideum, (i) proximal and (ii) distal view. The scale equals 10 cm.
Fig. 12. Éléments post-crâniens fossils d'*Alcicephalus neumayri* de Kavakdere. AV-245 : trapezoideo-capitatum droit en vue proximale (i) et distale (ii). B : PV-235, astragale droit en vues dorsale (i), latéral (ii), médiale (iii) et plantaire (iv). C : PV-238, naviculocuboideum droit en vues proximal (i) et distale (ii). Échelle = 10 cm.

Table 5
Measurements of post-cranial elements of *Alcicephalus neumayri* from Kavakdere. Sin: left; Dex: right; L: length; l: width; APD: antero-posterior diameter; TD: transverse diameter; prox: proximal; dis: distal; lat: lateral; med: medial; H: maximum height of the trapezoideo-capitatum; h: height of the articular surface for the scaphoideum; H1: Height of the cubonavicular on the level of the medial astragalar surface; H2: Height of the cubonavicular on the level of the lateral astragalar surface. All measurements given in millimetres.
Tableau 5
Mesures des éléments post-crâniens d'*Alcicephalus neumayri* de Kavakdere. Sin : gauche ; Dex : droite ; L : longueur ; l : largeur ; APD : diamètre antéro-postérieur ; TD : diamètre transversal ; prox : proximal ; dis : distal ; lat : latéral ; med : médial ; H : hauteur maximum du trapezoideo-capitatum ; h ; hauteur de la surface articulaire pour le scaphoideum ; H1 : hauteur du cubonaviculaire au niveau de la surface médiale de l'astragale ; H2 : hauteur du cubonaviculaire au niveau de la surface latérale de l'astragale. Toutes les mesures sont en millimètres.

Trapezoideo-capitatum

Inv. Number	Taxon	Sin/Dex	L	l	H	h
PV-245	*Alcicephalus neumayri*	dex	62.22	69.2	34.32	26.25

Astragalus

Inv. Number	Taxon	Sin/Dex	Llat	Lmed	TDprox	TDdis
PV-235	*Alcicephalus neumayri*	dex	100.6	85.25	67.36	65.5

Naviculocuboideum

Inv. Number	Taxon	Sin/Dex	TD	APDmed	APDmax	Hmax	H1	H2
PV-238	*Alcicephalus neumayri*	dex	93.93	71.02	86.03	55.98	25.62	35.94

The naviculocuboideum (PV-238; Fig. 12C) has a rectangle shape in proximal view. The astragalar facets are almost equally developed, with the medial facet being slightly narrower that the lateral one. The medial peak is short but is very prominent and has a sharp apex. The lateral pick is more robust and higher. The calcaneal facet is wide, and it is not extending behind the lateral peak, common feature of samotherines. In distal aspect, the facet for the metatarsal

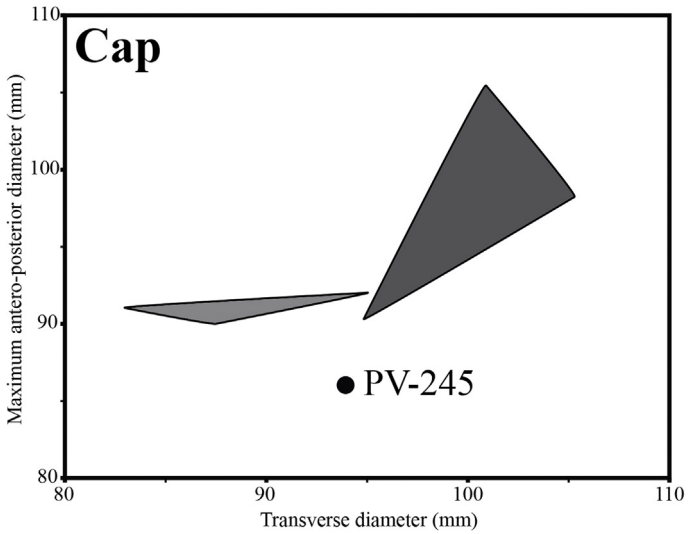
Cap
Maximum antero-posterior diameter (mm)
110
100
90
80
PV-245
80
90
100
110
Transverse diameter (mm)

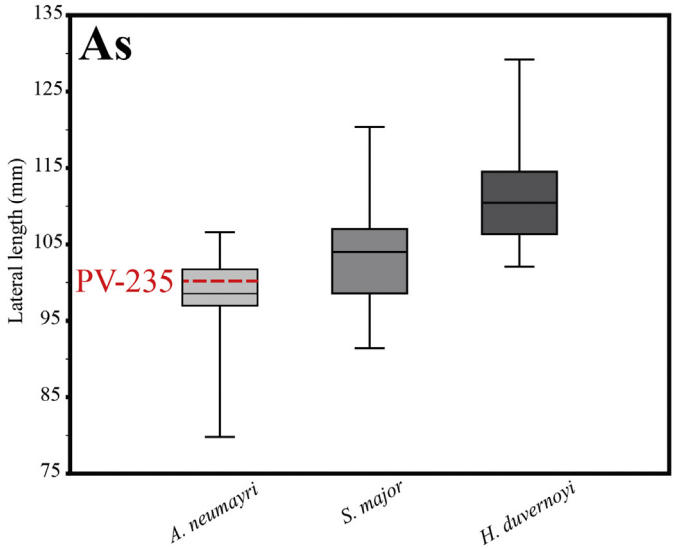
As
Lateral length (mm)
135
125
115
105
95
85
75
PV-235
A. neumayri
S. major
H. duvernoyi

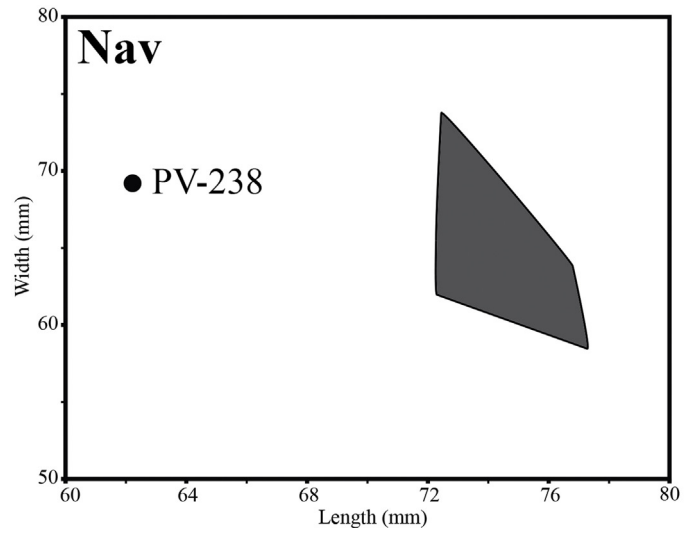
Nav
Width (mm)
80
70
60
50
PV-238
60
64
68
72
76
80
Length (mm)

Table 6
Measurements of astragali of *Alcicephalus neumayri* from Maragha. Sin: left; Dex: right; L: length; TD: transverse diameter; prox: proximal; dis: distal; lat: lateral; med: medial. All measurements given in millimetres.
Tableau 6
Mesures d'astragales d'*Alcicephalus neumayri* de Maragha. Sin ; gauche ; Dex : droite ; L : longueur ; TD : diamètre transversal ; prox : proximal ; dis : distal ; lat : latéral ; med : médial. Toutes les mesures sont en millimètres.

Inv. Number	Sin/Dex	Llat	Lmed	TDprox	TDdis
NHMW 2019/0018/0001	sin	100.95	90.26	71.49	65.04
NHMW 2019/0018/0002	sin	98.57	85.73	69.13	66.3
NHMW 2019/0018/0003	sin	105.55	93.26	64.9	68.4
NHMW 2019/0018/0004	dex	97.24	87.33	61.33	59.26

is wide and semi-circular in shape. There is a wide opening on the distal part of that surface, which suggests a strong insertion of the tendons of the digital flexor muscles leading towards the proximal metatarsal canal. The facet for the external cuneiform is notably smaller than the latter surface and sub-rectangle. The medial cuneiform facet is triangular and almost completely isolated from the facet of the external cuneiform.

Comparisons and remarks: *Alcicephalus neumayri* has been reported from its type locality, Maragheh, as well as from North China and it is the most frequently occurring giraffid at the easternmost border of the Pikermian biome (de Mecquenem, 1924-1925; Gaziry, 1987; Solounias and Danowitz, 2016b; Rodler and Weithofer, 1890). Due to the similarities between *Alcicephalus* and *Samotherium*, the two genera we considered synonymous for a long time (Hamilton, 1978; Simpson, 1945). However, a recent study by Hou et al. (2014) pointed out the cranial differences between the two genera and re-established *Alcicephalus* as a valid genus. Even though *A. neumayri* is mostly known from dental and cranial material, recent data published by Solounias and Danowitz (2016b), as well as new analyses (for this study) on unpublished material from Maragheh (hosted in the collections of NHMW), allowed for a detailed comparison with the astragalus from Kavakdere.

Metrical comparison of the post-cranial elements clearly separates the carpal and tarsal bones of *A. neumayri* from those of *S. major* and *H. duvernoyi* (Fig. 13). The trapezoideo-capitatum (PV-245), astragalus (PV-235) and naviculocuboideum (PV-238) clearly belong to a species smaller than *Helladotherium*. Morphologically, the trapezoideo-capitatum has an almost rectangle shape and blunt cranial crests, characters that are not only different from those of *H. duvernoyi* but also typical for samotheriines (Kostopoulos, 2009). Additionally, the naviculocuboideum displays a short calcanear facet, which in uncommon in Sivatheriinae (Kostopoulos, 2009; Nishioka et al., 2014; Solounias and Danowitz, 2016a). The medial astragalar facet is blunt, protruding only slightly, which is responsible for the faint intracephalic fossa of the astragalus. Lastly, the triangular facet for the medial cuneiform, as well as the fossa on the distal part of the facet for the metatarsal comprise unique characters on the naviculocuboideum of *A. neumayri*.

The astragalus constitutes a highly diagnostic skeletal element for Giraffidae. A recent study conducted by Solounias and Danowitz (2016a) described and listed all the different characters of the astragali of various giraffid taxa. In a late study, Solounias and Danowitz (2016b) showed the coexistence of *Alcicephalus neumayri* and *Samotherium major* at Maragheh, where the astragali are well described and the morphological differences between the two taxa were briefly indicated. Further investigation of the Maragheh collection hosted in NHMW, confirms the coexistence of two samotheriines at Maragheh. Additionally, a descent collection of astragali allowed to depict the morphological differences between the two taxa (Fig. 14).

In dorsal view, the astragalus of *A. neumayri* exhibits lateral edge which is notably taller but not much thicker that the medial ridge of the trochlea. In *Helladotherium* and *S. major*, the lateral ridge is much thicker than the medial one and, in the latter taxon, the two ridges do not exhibit such a height difference (Solounias and Danowitz, 2016a). Additionally, in *A. neumayri* there is a large and irregularly shaped central fossa, which indicatively expands laterally, between the lateral ridge of the trochlea and the lateral collum tali. The medial groove is very wide, bearing a robust medial bulge. The lateral collum tali is also quite broad without carrying a lateral notch. Respectively, in *S. major* the central fossa appears to be more rounded and placed centrally, at the base of the trochlear groove. The medial groove is also very open, with a much weaker medial bulge. The lateral collum tali is narrower than in *A. neumayri*, while bearing a well-developed lateral notch (Solounias

Fig. 13. Dispersion plots showing the relative size of carpal and tarsal bones of *Alcicephalus neumayri* from Kavakdere. The light grey areas represent the *Samotherium major* morphospaces. The dark grey areas represent the *Helladotherium duvernoyi* morphospaces. The circle points and the red dashed line represent the Kavakdere specimens. In the boxplot, each box represents 50% of the range of the premolar length, while the top and the bottom bars represent the overall range of the length. The horizontal line in the centre of each box represents the median of the sample. All measurements given in millimetres (data from Gaziry, 1987; Iliopoulos, 2003; Kostopoulos, 2009; Solounias and Danowitz, 2016b; personal data of AX).
Fig. 13. Diagramme de dispersion montrant la taille relative des os carpiens et tarsiens d'*Alcicephalus neumayri* de Kavakdere. Les zones en gris clair représentent les morpho-espaces de *Samotherium major* et les zones en gris foncé ceux d' *Helladotherium duvernoyi*. Les points noirs et la ligne rouge tiretée représentent les spécimens de Karakdere. Dans le *boxplot*, chaque boîte représente 50 % de la gamme de longueur de la prémolaire, tandis que les barres en haut et en bas représentent le total de la longueur. La ligne horizontale au centre de chaque boîte représente la moyenne de l'échantillonnage. Toutes les mesures sont en millimètres (données de Graziry, 1987 ; Iliopoulos, 2003 ; Kostopoulos, 2009 ; Solounias et Danowitz, 2016b ; données personnelles de AX).

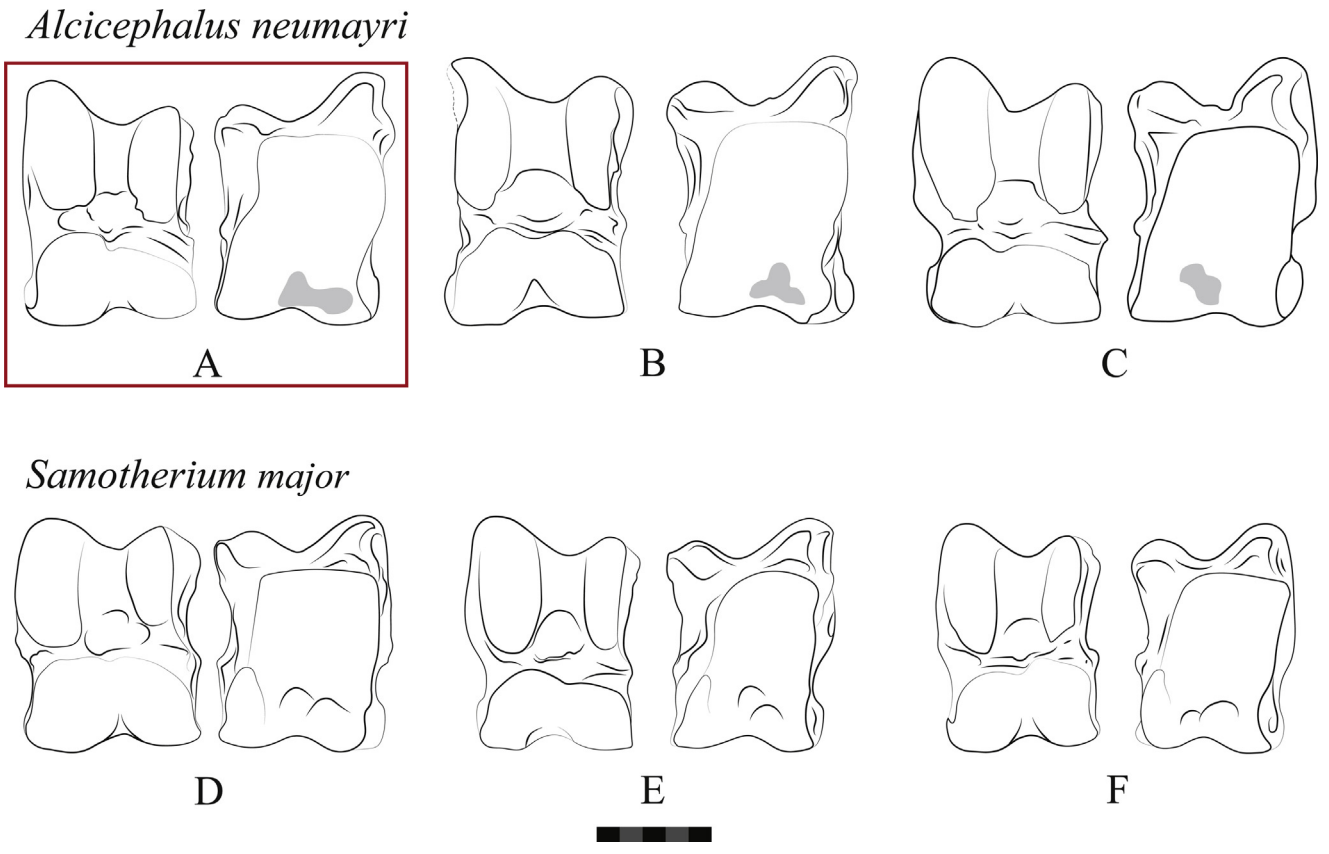

Fig. 14. Graphic demonstration of dorsal and plantar aspects of astragali of *Alcicephalus neumayri* and *Samotherium major*. A: PV-235; B: NHMW 2019/0018/0001; C: NHMW 2019/0018/0004; D: NHMW 2019/0017/0001; E: NHMW 2019/0017/0002; F: NHMW 2019/0017/0005. E and B are mirrored, in order to make the correspondence of the characters easier. *Alcicephalus neumayri* from Kavakdere is represented in the red box. The scale equals 5 cm.

Fig. 14. Démonstration graphique des aspects dorsal et plantaire des astragales d'*Alcicephalus neumayri* et de *Samotherium major*. A : PV-235 ; B : NHMW 2019/0018/0001 ; C : NHMW 2019/0018/0004 ; D : NHMW 2019/0017/0001 ; E : NHMW 2019/0017/0002 ; F : NHMW 2019/0017/0005. E and B sont représentés comme un reflet l'un de l'autre, de manière à ce que la correspondance des caractères soit plus facile à voir. *Alcicephalus neumayri* est représenté dans la boîte rouge. Échelle = 5 cm.

and Danowitz, 2016a). In plantar aspect, the astragali of *A. neumayri* exhibit an irregularly-shaped ventral articular surface. On the distal and lateral side, there is a characteristic concavity of the articular surface, while the medial scala has vague limits or is hardly visible. The distal intracephalic fossa exhibits a double depression, common character for samotherines (Solounias and Danowitz, 2016a). However, the limits of the fossae are hard to define. Correspondingly, the astragali of *S. major* show a more regular, rectangular shape of the ventral articular surface. The medial scala, even though weak, is distinct with determinable limits, and a characteristic and conspicuous double-sectioned distal intracephalic fossa is also present (Solounias and Danowitz, 2016a).

4. Discussion and conclusions

Up to date, few studies have been conducted on fossil remains from the fossiliferous horizons at Kavakdere. Ozansoy (1965) was the first to study fossil remains from Kavakdere, recognizing *Helladotherium* sp. and *Camelopardalis* sp. as the only two giraffid taxa. Later, Becker-Platen et al. (1975) updated the faunal list for Kavakdere, adding Giraffa sp. to the previously identified giraffid taxa. However, in both studies, the basis for their determination is unknown, since comprehensive descriptions and figures of the fossil material are missing. A study by Köhler (1987), focusing on Miocene bovids from Turkey also presented material of *Protoryx* sp. Forsyth-Major (1891) from Kavakdere, adding yet another taxon to the unclear ruminant list from this locality. The first real taxonomic study on fossil Giraffidae from Kavakdere was conducted by Geraads and Güleç (1999). These authors described an almost complete skull of *Bramatherium perimense*, hosted in MTA. The material described herein clarifies the taxonomic position of giraffid material from Kavakdere. It verifies the presence of *Bramatherium perimense* and provides evidence for four additional giraffid taxa, *H. duvernoyi*, *Palaeotragus rouenii*, *Samotherium boissieri*, and *Alcicephalus neumayri*.

Kavakdere was initially placed between the middle Vallesian and early Turolian by Ozansoy (1965) and later, ambiguously assigned to the MN11 zone by Köhler (1987). Based on new findings, Geraads and Güleç (1999) assigned Kavakdere to middle Turolian. Succeeding, the palaeomagnetic dating established by Kappelman et al. (2003) placed all Kavakdere localities within MN11.

Palaeotragus rouenii has a chronostratigraphic distribution that ranges between late Vallesian (MN10) and late Turolian (MN 13) (Gentry et al., 1999; Kostopoulos, 2009; Koufos et al., 2009). *Helladotherium duvernoyi* has also a wide distribution, which ranges from late Vallesian to late Turolian, with the first occurrence from the late Vallesian of Nikiti (Kostopoulos, 2009; Kostopoulos and Koufos, 2006; Kostopoulos et al., 1996; Koufos et al., 2009). *Bramatherium perimense* is known from both the MN10 and MN11 of Pakistan and Turkey, as well as from the type locality of Perim (Piram) Island, India (Falconer, 1845; Geraads and Güleç, 1999; Welcomme et al., 1997). However, the type horizon is unknown, and the exact age of the holotype is uncertain. *Samotherium boissieri* first appeared in the late Vallesian of Gülpınar and survived until the early middle Turolian (Marra et al., 2011). The taxon finds its peak of abundance in the MN11 where it appears as the dominant species of the famous locality Old Mills Beds, Samos, Greece (Bernor et al., 1996; Kostopoulos et al., 2003; Koufos et al., 1997).

So far, *Alcicephalus neumayri* has only been reported from localities at Maragheh, Iran (Bernor, 1986; Rodler and Weithofer, 1890), as well as China, and it is in fact the most abundant giraffid known from the eastern outskirts of the Pikermian biome (Solounias and Danowitz, 2016b). However, there is no exact indication regarding the stratigraphic origin of *A. neumayri*, giving the taxon a general chronostratigraphic range of lower to middle Turolian (MN11–MN12). The presence of *A. neumayri* in Kavakdere comprises the westernmost occurrence of this taxon and suggests a more dominant presence of *Alcicephalus* in the Pikermian biome than previously advocated.

Conclusively, most faunal remains of Giraffidae from Kavakdere agree with the chronostratigraphic conclusions of previous studies. In addition, the westernmost record of *A. neumayri* is reported. The new findings enrich the so-far limited fauna list of the fossiliferous site and new insights on the osteology of *Bramatherium* and *Alcicephalus* are documented.

Acknowledgements

We thank Y. Nishioka (Waseda Institute for Advanced Study) for kindly providing high-quality pictures of *Bramatherium* specimens from Thailand. Special thanks to U. B. Göhlich (NHMW) for granting A.X. access to fossil material from Maragheh. M. Aiglstorfer (Staatliches Museum für Naturkunde Stuttgart) and L. W. van den Hoek Ostende (Naturalis Biodiversity Center) are thanked for fruitful discussions on the material and the content of this manuscript. We owe thanks to the handling editor Dr. Lorenzo Rook for his assistance in the submission and review of the manuscript. We also kindly acknowledge the two anonymous reviewers for their comments and remarks, which considerably helped improving this publication. S.M., T.K., and K.H. were supported by Ege University, Izmir (research projects: TTM/001/2010, TTM/002/2011, TTM/001/2013, TTM/001/2014, TTM/001/2016, TTM/002/2016). A.X. and F.G. were funded by the Austrian Science Fund (FWF, project number P29501-B25).

References

Antoine, P.-O., Métais, G., Orliac, M.J., Crochet, J.-Y., Flynn, L.J., Marivaux, L., Rahim Rajpar, A., Roohi, G., Welcomme, J.-L., 2013. Mammalian Neogene biostratigraphy of the Sulaiman Province, Pakistan. In: Wang, X., Flynn, L.J., Fortelius, M. (Eds.), Fossil Mammals of Asia. Neogene Biostratigraphy and Chronology. Columbia University Press, New York, pp. 400–422.

Arambourg, C., 1963. Continental vertebrate faunas of the Tertiary of North Africa. In: Howell, F.C., Bourlière, F. (Eds.), African ecology and human evolution. Aldine Publication Co, Chicago, pp. 56–63.

Athanassiou, A., 2002. Neogene and Quaternary mammal faunas of Thessaly. Ann. geol. Pays hellen. 39 (A), 279–293.

Bakalov, P., Nikolov, I.V., Tzankov, V., 1962. Les Fossiles de Bulgarie. X. Mammifères tertiaires. Académie des sciences de Bulgarie, Sofia (In Bulgarian with French abstract).

Bärmann, E.V., Rössner, G.E., 2011. Dental nomenclature in Ruminantia: Towards a standard terminological framework.

Mammalian Biology-Zeitschrift für Säugetierkunde 76 (6), 762–768, http://dx.doi.org/10.1016/j.mambio.2011.07.002.
Becker-Platen, J.D., Sickenberg, O., Tobien, H., 1975. Vertebraten-Lokalfaunen der Türkei und ihre Altersstellung. In: Sickenberg, O. (Ed.), Die Gliederung des höheren Jungtertiärs und Altquartärs in der Türkei nach Vertebraten und ihre Bedeutung für die internationale Neogen-Stratigraphie (Känozoikum und Braunkohlen der Türkei. 17.). Geol. Jahrbuch (Regionale Geologie Ausland), Reihe B, 15, Hannover, pp. 47–100.
Bernor, R.L., 1986. Mammalian biostratigraphy, geochronology, and zoogeographic relationships of the Late Miocene Maragheh fauna, Iran. J. Vert. Paleontol. 6, 76–95.
Bernor, R.L., Solounias, N., Swisher III, C.C., van Couvering, J.A., 1996. The correlation of the classical "Pikermian" mammal faunas - Maragheh, Samos and Pikermi, with the European MN unit system. In: Bernor, R.L., Fahlbusch, V., Mittmann, H.W. (Eds.), The Evolution of the Western Eurasian Neogene Mammal Faunas. Columbia University Press, New York, pp. 137–154.
Bhatti, Z.H., Khan, M.A., Akhtar, M., 2012. *Hydaspitherium* (Artiodactyla: Giraffidae) from the Dhok Pathan Formation of the Middle Siwaliks, Pakistan: New Collection. Pakistan J. Zool 44 (3), 799–808.
Bibi, F., Hill, A., Beech, M., Yasin, W., 2013. Late Miocene fossils from the Baynunah Formation. In: Wang, X., Flynn, L.J., Fortelius, M. (Eds.), Fossil Mammals of Asia: Neogene Biostratigraphy and Chronology. Columbia University Press, New York, pp. 583–594.
Bohlin, B., 1926. Die Familie Giraffidae mit besonderen Berucksichtgung der fossilen Formen aus China. Palaeontologia Sinica, ser C. 4. The Geological Survey of China, Peking.
Bonis, L.D., Bouvrain, G., Geraads, D., Koufos, G.D., 1992. Diversity and paleoecology of Greek late Miocene mammalian faunas. Palaeogeogr. Palaeoclimatol. Palaeoecol. 91 (1–2), 99–121, http://dx.doi.org/10.1016/0031-0182(92)90035-4.
Borissiak, A., 1914. Mammifères fossiles de Sébastopol II. Mémoires du Comité géologique, Nouvelle série. Livraison 137, Paris.
Brunet, M., Heintz, E., Sen, S., 1981. Datations paléontologiques et séquences biochronologiques dans le Néogène continental d'Afghanistan. C. R. Acad. Sci. Paris, Ser. III 293, 305–308.
Colbert, E., 1935. Siwalik Mammals in the American Museum of Natural History. Trans. Am. Phil. Soc. 26, 1–401, http://dx.doi.org/10.2307/1005467.
Danowitz, M., Sukuan, H., Mihlbachler, M., Hastings, V., Solounias, N., 2016. A combined-mesowear analysis of late Miocene giraffids from North Chinese and Greek localities of the Pikermian Biome. Palaeogeogr. Palaeoclimatol. Palaeoecol. 449, 194–204, http://dx.doi.org/10.1016/j.palaeo.2016.02.026.
De Mecquenem, R., 1924-1925. Contribution à l'étude des fossiles de Maragha. Ann. Paleontol. 13–14, 135–160.
Falconer, H., 1845. Description of some fossil remains of *Dinotherium*, giraffe and other Mammalia, from the Gulf of Cambay, Western Coast of India. Quart. J. Geol. Soc. Lond. I, 356–372.
Forsyth-Major, C.J., 1888. Sur un gisement d'ossements fossiles dans l'île de Samos contemporains de l'âge de Pikermi. C. r. hebd. Séances Soc. geol. France 107, 1178–1181, http://dx.doi.org/10.1017/S0016756800189356.
Forsyth-Major, C.J., 1891. Considérations nouvelles sur la faune de vertébrés du Miocène supérieur dans l'île de Samos. C. r. hebd. Séances Soc. geol. France 113, 608–610.
Gaillard, C., 1899. Mammifères miocènes de la Grive-Saint-Alban (Isère). Arch. Mus. Hist. Nat. Lyon. 7, 1–41.
Gaudry, A., 1860. Résultats des fouilles executées en Grèce sous les auspices de l'Academie. C. r. hebd. séances Acad. sci. 51, 802–804.
Gaudry, A., 1861. Note sur la giraffe et l'*Helladotherium* trouvées à Pikermi (Grèce). Bull. Soc. geol. France, 2e Ser. 5, 587–597.
Gaudry, A., Lartet, E., 1856. Résultats des recherches paléontologiques entreprises dans l'Attique sous les auspices de l'Académie. C. r. hebd. séances Acad. sci. 43, 271–274.
Gaur, R., Vasishat, R.N., Chopra, S.R.K., 1985. New and some additional fossil mammals from the Siwaliks exposed at Nurpur, Kangra District (H.P.), India, with remarks on Siwalik giraffids. J. Palaeontol. Soc. India 30, 42–48.
Gaziry, A.W., 1987. Fossile Giraffen-Extremitäten aus Maragheh/Iran. Mitteilungen aus dem geologisch-paläontologischen Institut der Universität Hamburg 63, 185–199.
Gentry, A.W., 2003. Ruminantia (Artiodactyla). In: Fortelius, M., Kappelman, J., Sen, S., Bernor, R.L. (Eds.), Geology and Paleontology of the Miocene Sinap Formation, Turkey. Columbia University Press, New York, pp. 332–379.
Gentry, A.W., Heizmann, E.P.J., 1996. Miocene Ruminants of the Central and Eastern Tethys and Paratethys. In: Bernor, R.L., Fahlbusch, V., Mittmann, H.W. (Eds.), The evolution of Western Eurasian Neogene mammal faunas. Columbia University Press, New York, pp. 379–391.
Gentry, A.W., Rössner, G.E., Heizmann, E.P.J., 1999. Suborder Ruminantia. In: Rössner, G.E., Heissig, K. (Eds.), The Miocene land mammals of Europe. Verlag Dr. Friedrich Pfeil, Munich, pp. 225–253.
Geraads, D., 1974. Les Giraffidés du Miocène supérieur de la région de Thessalonique (Grèce). Unpublished PhD Thesis, University of Paris, France.
Geraads, D., 1986. Remarques sur la systématique et la phylogénie des Giraffidae (Artiodactyla, Mammalia). Geobios 19 (4), 465–477, http://dx.doi.org/10.1016/s0016-6995(86)80004-3.
Geraads, D., 1994. Les gisements de mammifères du Miocène supérieur de Kemiklitepe, Turquie. VIII: Giraffidae. Bull. Mus. natl hist. nat. Section C Sci. Terre Paleontol. Geol. Mineral. 16 (1), 159–173.
Geraads, D., Güleç, E., 1999. A *Bramatherium* skull (Giraffidae, Mammalia) from the late Miocene of Kavakdere (Central Turkey). Bull. Min. Res. Explor. 121, 51–56.
Geraads, D., Spassov, N., Kovachev, D., 2005. Giraffidae (Artiodactyla, Mammalia) from the Late Miocene of Kalimantsi and Hadjidimovo, Southwestern Bulgaria. Geol. Balc. 35 (1–2), 11–18.
Godina, A.Y., 1979. History of fossil giraffes of the genus Palaeotragus. Trudy, 177. Paleontological Institut Akademia Nauk USSR (In Russian).
Gray, J.E., 1821. On the natural arrangement of vertebrose animals. Lond. Med. Rep. 15, 297–310.
Grossman, A., Solounias, N., 2014. New fossils of Giraffoidea (Mammalia: Artiodactyla) from the Lothidok Formation (Kalodirr Member, early Miocene, West Turkana, Kenya) contribute to our understanding of early giraffoid diversity. Zitteliana B 32, 63–70, http://dx.doi.org/10.5282/ubm/epub.22387.
Hamilton, W.R., 1978. Fossil giraffes from the Miocene of Africa and a revision of the phylogeny of the Giraffoidea. Phil. Trans. R. Soc. B. 283, 165–229.
Hammer, Ø., Harper, D.A.T., Ryan, P.D., 2001. PAST: Palaeontological Statistics software package for education and data analysis. Palaeontol. Electr. 4, 1–9 http://palaeo-electronica.org/2001_1/past/past.pdf.
Harris, J., Solounias, N., Geraads, D., 2010. Giraffoidea. In: Werdelin, L., Sanders, W.J. (Eds.), Cenozoic Mammals of Africa. University of California Press, Berkeley, CA, USA, pp. 797–811, http://dx.doi.org/10.1525/california/9780520257214.003.0039.
Hensel, R., 1862. Über die Reste einiger Säugethierarten von Pikermi in der Münchener Sammlung. Mber. K. Preuss. Akad. Wiss. 27, 560–569.
Hou, S., Danowitz, M., Sammis, J., Solounias, N., 2014. Dead ossicones, and other characters describing Palaeotraginae (Giraffidae; Mammalia) based on new material from Gansu, Central China. Zitteliana 32, 91–98.
Iliopoulos, G., 2003. The Giraffidae (Mammalia, Artiodactyla) and the study of the histology and chemistry of fossil mammal bone from the late Miocene of Kerassia (Euboea Island, Greece), Unpublished PhD Thesis, University of Leicester, UK. http://hdl.handle.net/2381/35044.
Janis, C.M., 1987. Grades and clades in hornless ruminant evolution: the reality of the Gelocidae and the systematic position of *Lophiomeryx* and *Bachitherium*. J. Vert. Paleontol. 7 (2), 200–216, http://dx.doi.org/10.1080/02724634.1987.10011653.
Kappelman, J., Duncan, A., Feseha, M., Lunkka, J.-P., Ekhardt, D., McDowell, F., Ryan, T.M., Swisher, C.C., 2003. Chronology. In: Fortelius, M., Kappelman, J., Sen, S., Bernor, R.L. (Eds.), Geology and Paleontology of the Miocene Sinap Formation, Turkey. Columbia University Press, New York, pp. 41–66.
Karadenizli, L., Seyitoğlu, G., Sen, S., Arnaud, N., Kazancı, N., Saraç, G., Alçiçek, C., 2005. Mammal Bearing Late Miocene Tuffs of the Akkasdagi Region; Distribution, Age, Petrographical and Geochemical Characteristics. In: Sen, S. (Ed.), Geology, Mammals and Environments at Akkaşdağı, Late Miocene of Central Anatolia, 27. Geodiversitas, pp. 553–566.
Khan, M.A., Akhtar, M., Irum, A., 2014. *Bramatherium* (Artiodactyla, Ruminantia, Giraffidae) from the Middle Siwaliks of Hasnot, Pakistan: biostratigraphy and palaeoecology. Turkish J. Earth Sci. 23 (3), 308–320.
Köhler, M., 1987. Boviden des türkischen Miozäns (Känozoikum und Bräunkohlen der Türkei). Paleontologia i Evolucio 21, 133–246.
Köhler, M., Moya-Sola, S., Morales, J., 1995. The vertebrate locality Maramena (Macedonia, Greece) at the Turolian-Ruscinian boundary (Neogene), 15. Bovidae and Giraffidae (Artiodactyla, Mammalia). Münch. geowiss. Abh. A Geol. Paläontol. 28, 167–180.
Koken, E., 1885. Über fossile Säugethiere aus China. Palaeontol. Abh. 3, 31–113.
Kostopoulos, D.S., Koufos, G.D., 2006. The late Miocene vertebrate locality of Perivolaki, Thessaly, Greece. 8. Giraffidae. Palaeontographica Abteilung A 276 (1–6), 135–149.

Kostopoulos, D.S., Saraç, G., 2005. Giraffidae (Mammalia, Artiodactyla) from the late Miocene of Akkaşdağı, Turkey. In: Sen, S. (Ed.), Geology, mammals and environments at Akkaşdağı, late Miocene of Central Anatolia, 27. Geodiversitas, pp. 735–745.
Kostopoulos, D.S., Koufos, G.D., Sylvestrou, I.A., Syrides, G.E., Tsompachidou, E., 2009. 2. Lithostratigraphy and Fossiliferous Sites. In: Koufos, G.D., Nagel, D. (Eds.), The Late Miocene Mammal Faunas of the Mytilinii Basin, Samos Island, Greece: new Collection. Beitr. Palaeontol., 31. Vienna, Austria, pp. 13–26.
Kostopoulos, D.S., Koliadimou, K.K., Koufos, G.D., 1996. The giraffids (Mammalia, Artiodactyla) from the late Miocene mammalian localities of Nikiti (Macedonia, Greece). Palaeontogr. Abt. A 239 (1–3), 61–88.
Kostopoulos, D.S., Sen, S., Koufos, G.D., 2003. Magnetostratigraphy and revised chronology of the late Miocene mammal localities of Samos. Greece. Int. J. Earth Sci. 92 (5), 779–794, http://dx.doi.org/10.1007/s00531-003-0353-8.
Kostopoulos, D.S., 2009. 13. Giraffidae. In: Koufos, G.D., Nagel, D. (Eds.), The late Miocene mammal faunas of the Mytilinii Basin, Samos Island, Greece: new collection, Beitr. Palaeontol., 31. Vienna, Austria, pp. 299–343.
Koufos, G.D., 1990. The hipparions of the lower Axios valley (Macedonia, Greece). Implications for the Neogene stratigraphy and the evolution of hipparions. In: Lindsay, E.H., Fahlbusch, V., Mein, P. (Eds.), European Neogene Mammal Chronology. NATO ASI Series (Series A: Life Sciences), Springer, Boston, MA, USA, 180, pp. 321–338, http://dx.doi.org/10.1007/978-1-4899-2513-8_19.
Koufos, G.D., 2006. The Neogene mammal localities of Greece: faunas, chronology and biostratigraphy. Hellenic J. Geosci. 41 (1), 183–214.
Koufos, G.D., Kostopoulos, D.S., Vlachou, T.D., 2009. 16. Biochronology. In: Koufos, G.D., Nagel, D. (Eds.), The late Miocene mammal faunas of the Mytilinii basin, Samos Island, Greece: new collection. Beitr. Palaeontol., 31. Vienna, Austria, pp. 397–408.
Koufos, G.D., Syrides, G., Kostopoulos, D.S., Koliadimou, K.K., Sylvestrou, I., Stefanides, G., Vlachou, D., 1997. New excavations in the Neogene mammalian localities of Mytilinii, Samos island, Greece. Geodiversitas 19 (4), 877–885.
Koufos, G.D., Mayda, S., Kaya, T., 2018. New carnivoran remains from the late Miocene of Turkey. Palaeontol. Z. 92 (1), 131–162.
Lewis, G.E., 1939. A new *Bramatherium* skull. Am. J. Sci. 237 (4), 275–280.
Linnaeus, C., 1758. Systema Naturae, 1., 10 ed. Engelman, Leipzig.
Lunkka, J.-P., Kappelman, J., Ekart, D., Crabaugh, J., Gibbard, P., 2003. Geology. In: Fortelius, M., Kappelman, J., Sen, S., Bernor, R.L. (Eds.), Geology and Paleontology of the Miocene Sinap Formation, Turkey. Columbia University Press, New York, pp. 25–40.
Lydekker, R., 1876. Indian Tertiary and Post-Tertiary Vertebrata. Descriptions of the molar teeth and other remains of Mammalia. Mem. Geol. Surv. India. 1, 19–83.
Lydekker, R., 1878. Crania of Ruminants from the Indian Tertiaries. Palaeontol. Indica 10, 88–171.
Marinos, G., Symeonidis, N., 1974. Neue Funde aus Pikermi (Attika, Griechenland) und eine allgemeine geologische Übersicht dieses paläontologischen Raumes. Ann. Geol. Pays hellen. 26, 1–20.
Marra, A.C., Solounias, N., Carone, G., Rook, L., 2011. Palaeogeographic significance of the giraffid remains (Mammalia, Arctiodactyla) from Cessaniti (Late Miocene, Southern Italy). Geobios 44 (2–3), 189–197.
Matthew, W.D., 1929. Critical observations upon Siwalik mammals. Bull. Am. Mus. Nat. Hist. 56, 437–560.
Nishioka, Y., Hanta, R., Jintasakul, P., 2014. Note on giraffe remains from the Miocene of continental Southeast Asia. J. Sci. Technol. MSU. 33 (4), 365–377.
Owen, R., 1848. Description of teeth and portions of jaws of two extinct anthracotherioid quadrupeds (Hyopotamus vectianus and Hyop. bovinus) discovered by the Marchioness of Hastings in the Eocene deposits on the N.W. coast of the Isle of Wight: with an attempt to develop Cuvier's idea of the classification of pachyderms by the number of their toes. Quart. J. Geol. Soc. London 4, 103–141, http://dx.doi.org/10.1144/gsl.jgs.1848.004.01-02.21.
Ozansoy, F., 1965. Étude des gisements continentaux et des mammifères du Cénozoïque de Turquie. Mem. Soc. geol. France 102, 1–93.
Pilgrim, G.E., 1911. The Fossil Giraffidae of India. Mem. Geol. Surv. India. 4, 1–29.
Raza, S.M., Cheema, I.U., Downs, W.R., Rajpar, A.R., Ward, S.C., 2002. Miocene stratigraphy and mammal fauna from the Sulaiman Range, Southwestern Himalayas, Pakistan. Paleogeogr. Palaeoclimatol. Palaeoecol. 186 (3–4), 185–197.
Ríos, M., Danowitz, M., Solounias, N., 2016. First comprehensive morphological analysis on the metapodials of Giraffidae. Palaeontol. Electr. 19 (3), 1–39.
Rodler, A., Weithofer, K.A., 1890. Die Wiederkäuer der Fauna von Maragha. Denkschr. Kaiserl. Akad. Wiss. Wien 57, 753–772.
Roth, J., Wagner, A., 1854. Die fossilen Knochenüberreste von Pikermi in Griechenland. Abh. Bayer. Akad. Wiss., Math.-phys. Kl. 7, 371–464.
Roussiakis, S., Iliopoulos, G., 2004. Preliminary observations on the metrical variation of *Helladotherium duvernoyi* and *Bohlinia attica* , In: 5th International Symposium on Eastern Mediterranean Geology, Thessaloniki, pp. 343–346.
Saraç, G., 2003. Turkiye omurgali fosil yataklari. Mineral Res. Expl. Direct. Turkey (MTA). Scientific Report No: 10609, Ankara, Turkey (in Turkish).
Schaller, O., 2007. Illustrated Veterinary Anatomical Nomenclature, 2nd ed. Enke Verlag, Stuttgart, Germany, http://dx.doi.org/10.1024/0036-7281.149.9.417c.
Sehgal, R.K., 2015. Mammalian faunas from the Siwalik sediments exposed around Nurpur, District Kangra (HP): age and palaeobiogeographic implications. Himalayan Geol. 36 (1), 9–22.
Sehgal, R.K., Nanda, A.C., 2002a. Palaeoenvironment and palaeoecology of the Lower and middle Siwalik Subgroups of a part of Northwestern Himalaya. J. Geol. Soc. India 59 (6), 517–529.
Sehgal, R.K., Nanda, A.C., 2002b. Age of the fossiliferous Siwalik sediments exposed in the vicinity of Nurpur, District Kangra. Himachal Pradesh. Curr. Sci. 82 (4), 392–395.
Sen, S., 2003. History of Paleontologic Research in Neogene Deposits of the Sinap Formation, Ankara, Turkey. In: Fortelius, M., Kappelman, J., Sen, S., Bernor, R.L. (Eds.), Geology and Paleontology of the Miocene Sinap Formation, Turkey. Columbia University Press, New York, pp. 1–22.
Sen, S., 2017. What Kavakdere (Ankara) Late Miocene Mammals Bring to the Knowledge of Mammalian Evolution in Anatolia? , 15th Congress of the RCMNS, Exploring a “physical laboratory”: The Mediterranean Basin, Athens, Book of Abstracts, p. 145.
Şenyürek, M.S., 1954. A study of the remains of *Samotherium* found at Taskınpasa, Ankara Universitesi Dil ve Tahir-Cografya. Fakültesi Dergisi. 12 (1–2), 1–32, http://dx.doi.org/10.1501/dtcfder_0000001064.
Simpson, G.G., 1945. The principles of classification and a classification of mammals. Bull. Am. Mus. Nat. Hist. 85, 1–350.
Solounias, N., 1981a. The Turolian fauna from the island of Samos, Greece, with special emphasis on the hyaenids and the bovids. Contrib. Vertebr. Evol. 6, 1–232, http://dx.doi.org/10.1017/s0016756800026388.
Solounias, N., 1981b. Mammalian fossils of Samos and Pikermi. Part 2. Resurrection of a classic Turolian fauna. Ann. Carnegie Museum. 50, 231–270.
Solounias, N., 1988. Prevalence of ossicones in Giraffidae (Artiodactyla, Mammalia). J. Mammal. 69 (4), 845–848, http://dx.doi.org/10.2307/1381645.
Solounias, N., 2007. Family Giraffidae. In: Prothero, D.R., Foss, S.E. (Eds.), The evolution of artiodactyls,. The Johns Hopkins University Press, Baltimore, MD, USA, pp. 257–291.
Solounias, N., Danowitz, M., 2016a. Astragalar Morphology of Selected Giraffidae. Plos One 11 (3), e0151310, http://dx.doi.org/10.1371/journal.pone.0151310.
Solounias, N., Danowitz, M., 2016b. The Giraffidae of Maragheh and the identification of a new species of Honanotherium. In: Mirzaie Ataabadi, M., Fortelius, M. (Eds.), The late Miocene Maragheh mammal fauna; results of recent multidisciplinary research. Paleobiodivers. Paleoenviron. 96(3). , pp. 489–506, http://dx.doi.org/10.1007/s12549-016-0230-7.
Solounias, N., Plavcan, J.M., Quade, J., Witmer, L., 1999. The paleoecology of the Pikermian biome and the savanna myth. In: Agustí, J., Rook, L., Andrews, P. (Eds.), The Evolution of Neogene Terrestrial Ecosystems in Europe. , pp. 436–453.
Thomas, H., Sen, S., Ligabue, G., 1980. La faune miocene de la formation Agha Jari du Jebel Hamrin. Irak. Proc. K. Ned. Akad. Wet. 83, 269–287.
Viranta, S., Werdelin, L., 2003. Carnivora. In: Fortelius, M., Kappelman, J., Sen, S., Bernor, R.L. (Eds.), Geology and paleontology of the Miocene Sinap Formation. Columbia University Press, New York, pp. 178–193.
Welcomme, J.L., Antoine, P.O., Duranthon, F., Mein, P., Ginsburg, L., 1997. Nouvelles découvertes de Vertébrés miocènes dans le synclinal de Dera Bugti (Balouchistan, Pakistan). C.R. Acad. Sci. Paris, Ser. IIa 325 (7), 531–536.
Zdansky, O., 1924. Jungtertiäre Carnivoren chinas. Paleontol. Sin. C 2, 38–45.
Zittel, K.A., 1893. Handbuch der Paläontologie. Vertebrata (Mammalia), Vol. 4. R. Oldenbourg, Munich and Leipzig, Germany.